Electronic Supplementary Material (ESI) for ChemComm.

Supporting Information

“Give Me Five” - An Amino Imidazoline-2-imine Ligand Stabilises First Neutral Five-membered Cyclic Triel(I) Carbenoides

Lars Denker, Bartosz Trzaskowski,* and René Frank*

1 General Information

All procedures were performed under dry nitrogen atmosphere in a glove box (MBraun 200B) or using Schlenk techniques unless stated otherwise. Solvents were purified and dried using a Solvent Purification System (MBraun) and stored over sodium or potassium, except for halogenated solvents, which were stored over molecular sieves (3-4 Å). C_6D_6 and THF-D_8 were dried over sodium potassium alloy, filtered and stored under nitrogen. CD_2Cl_2 and $CDCl_3$ were dried over CaH_2, distilled and stored under nitrogen. All commercially available compounds (Sigma Aldrich, deutero, abcr, TCI) were used without further purification. The compoundsInCp* [1], GaCp* [2] [AlCp*]$_4$ [3], TlCp [4], $TlBF_4$ [5], KBn [6], S=C(N*i*PrCMe)$_2$, :C(N*i*PrCMe)$_2$ [7] were prepared according to literature methods.

NMR spectra were recorded on Bruker Avance II-300, Avance III-HD, Avance III-400 and AVII-600 spectrometers. The chemical shifts (δ) are reported in parts per million (ppm). The residual solvents peak (C_6D_5H, δ = 7.16 ppm; C_7D_7H δ = 7.00 ppm, THF-D_7H, δ = 3.58, 1.72 ppm; $CHCl_3$, δ = 7.16 ppm; $CDHCl_2$, δ = 5.32 ppm) is used for referencing of the ^{1}H spectra. The ^{13}C spectra are internally calibrated by using the ^{13}C resonances of the solvent peaks (C_6D_6, δ = 128.06 ppm; THF-D_8, δ = 67.21, 25.31 ppm; $CDCl_3$, δ = 77.16 ppm; CD_2Cl_2, δ = 53.84 ppm). For ^{11}B-NMR spectra an external calibration with $BF_3\cdot Et_2O$ was used. Coupling constants are stated in Hertz (Hz), multiplicities are defined as broad (br), singlet (s), doublet (d), triplet (t), septet (sept), multiplet (m), doublet of doublets (dd), doublet of doublet of doublets (ddd) or triplet of doublets (td).

If necessary, 2D-NMR experiments (H,H COSY, H,C HSQC, HC HMBC, H,N HMBC) were used to aid the assignment of the signals.

Elemental analyses were accomplished by combustion and gas chromatographic analysis using a VarioMICRO Tube and HW detection. Values are reported in weight-%.

2 Syntheses

2.1 *N*-(2,6-diisopropylphenyl)phenylene-1,2-diamine

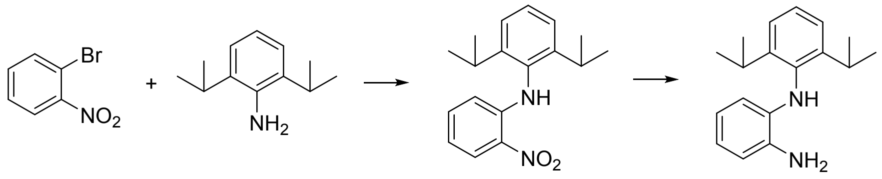

2a **2b** **2c** **2**

Intermediate **2c** [8]: Compound **2a** (5.0 g, 24.8 mmol, 1.0 eq.), Cs_2CO_3 (10.0 g, 31 mmol, 1.25 eq.), *rac*-BINAP (463 mg, 0.74 mmol, 3 mol%) and $Pd_2(dba)_3$ (283 mg, 0.31 mmol, 1.25 mol%) were dissolved in toluene (100 mL). Compound **2b** (5.0 mL, 24.8 mmol, 1.0 eq.) was added and the reaction mixture was stirred under reflux for 24 h. After cooling the solution was washed with water in air. The aqueous layer was extracted with DCM (3 × 200 mL) and the combined organic layers were dried over Mg_2SO_4. The solvents were removed under reduced pressure. The residue was purified via flash chromatography (1:1 DCM/PE) to yield product **2c** (6.91 g, 23.1 mmol, 94 %) as an orange solid.

^1H NMR (300 MHz, $CDCl_3$): δ (ppm) = 9.19 (s, 1 H, N*H*), 8.21 (dd, *J* = 8.6, 1.6 Hz, 1 H, *H* ortho to NO_2), 7.36 (dd, *J* = 8.5, 6.8 Hz, 1 H, *H* meta to NO_2), 7.30 – 7.20 (m, 3 H, aryl C−*H* in Dipp), 6.66 (ddd, *J* = 8.4, 6.9, 1.3 Hz, 1 H, *H* para to NO_2), 6.36 (dd, *J* = 8.6, 1.3 Hz, 1 H, *H* ortho to NH-Dipp), 3.02 (sept, *J* = 6.9 Hz, 2 H C*H*), 1.15 (d, *J* = 6.8 Hz, 6 H, $CH(CH_3)_2$), 1.09 (d, *J* = 6.9 Hz, 6 H, $CH(CH_3)_2$)).

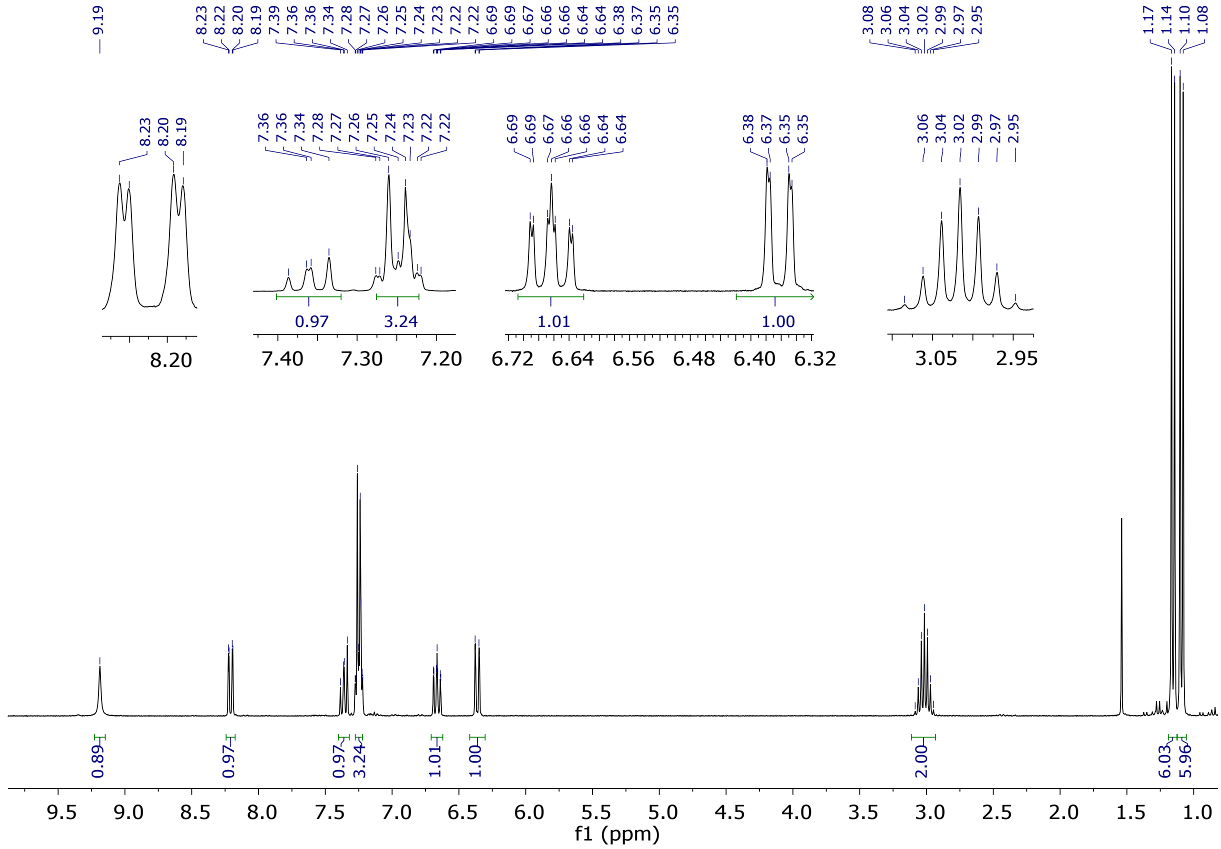

Figure S1: ^{1}H NMR spectrum of compound **2c**, (300 MHz, $CDCl_3$, 25 °C).

N-(2,6-diisopropylphenyl)phenylene-1,2-diamine **2** [9]: Compound **2c** (6.67 g, 22.4 mmol, 1.0 eq.) was dissolved in anhydrous THF (200 mL) and 5 % Pd/C (400 mg) was added to the solution. The suspension was stirred vigorously under 1 atm H_2. The H_2 atmosphere was renewed several times until the yellowish color of the suspension was discharged. The solution was filtered over Celite® and the solvent was removed *in vacuo* to give the product (5.81 g, 21.6 mmol, 97 %) as a grey solid.

^1H NMR (300 MHz, $CDCl_3$): δ (ppm) = 7.35 – 7.20 (m, 3 H, aryl C–*H* in Dipp), 6.83 (dd, *J* = 7.5, 1.7 Hz, 1 H, *H* ortho to NH_2), 6.75 (td, *J* = 7.4, 1.6 Hz, 1 H, *H* meta to NH-Dipp), 6.68 (td, *J* = 7.5, 1.8 Hz, 1 H, *H* meta to NH_2), 6.23 (dd, *J* = 7.7, 1.6 Hz, 1 H, *H* ortho to NH_2), 4.94 (s, 1 H, N*H*), 3.61 (s, 2 H, NH_2), 3.11 (sept, *J* = 6.9 Hz, 2 H, C*H*), 1.18 (s, 12 H, CH(CH_3)$_2$)).

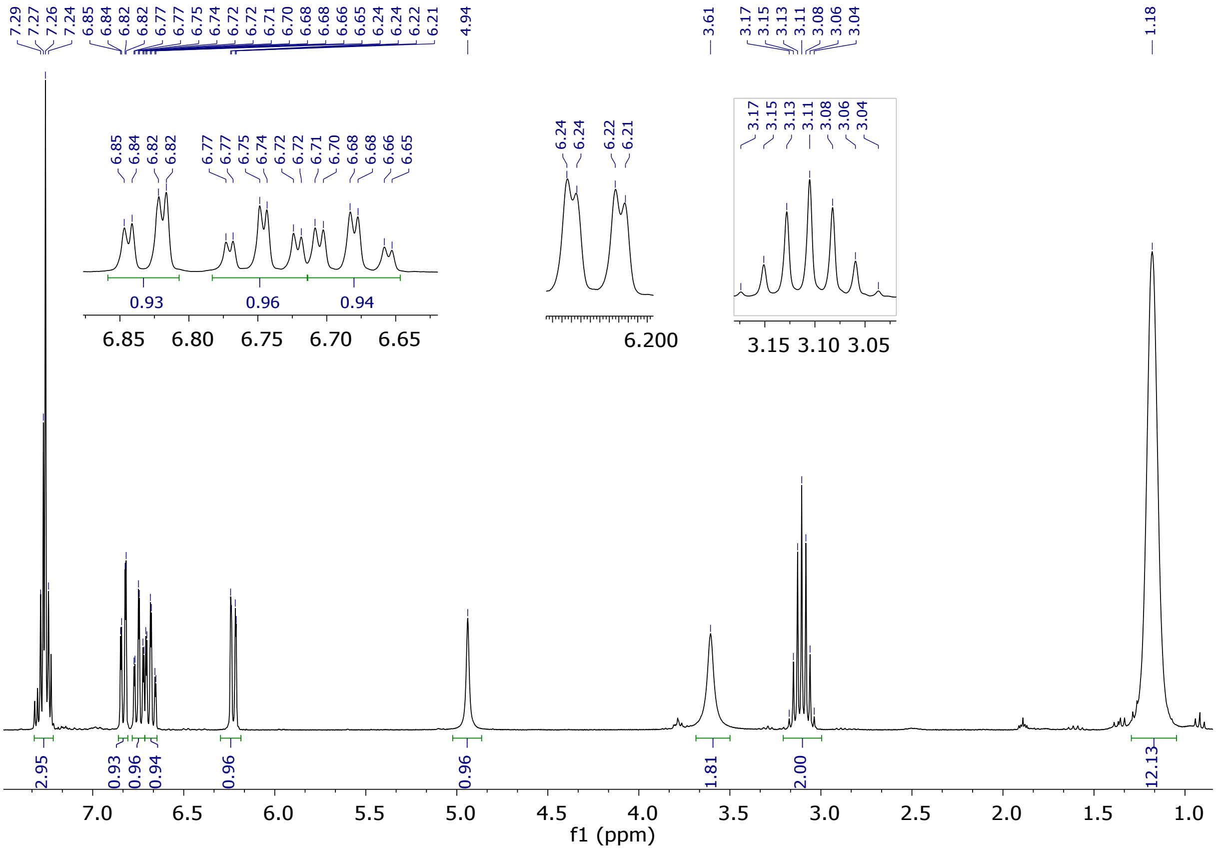

Figure S2: ^1H NMR spectrum of compound **2**, (300 MHz, $CDCl_3$, 25 °C).

2.2 2-Chloro-1,3-diisopropyl-4,5-dimethylimidazolium tetrafluoroborate [10]

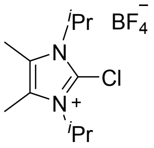

3

A portion of carbene [:C(N*i*PrCMe)$_2$, 5.0 g, 27.4 mmol, 1.0 eq.] was dissolved in THF (75 mL) and hexachloroethane (7.14 g, 30.2 mmol, 1.0 eq.) was added while stirring vigorously. The solution was stirred for 2 h while it was allowed to warm slowly to 25 °C. After stirring for 18 h at 25 °C the solution was treated with toluene (75 mL) and a precipitate was formed. The subsequent manipulations were performed in air. The precipitate was filtered over Celite® and was washed with toluene (2 × 25 mL). The product Celite® mixture was extracted with $CHCl_3$ (100 mL). The solution was washed with a $NaBF_4$ solution (5 g of $NaBF_4$ in 100 mL water). The aqueous layer was extracted with $CHCl_3$ (2 × 50 mL) and the combined organic layers were evaporated under reduced pressure. The residue was recrystallized from EtOAc/MeOH (20:1) to give the product (6.45 g, 21.3 mmol, 78 %) as an off-white solid **3**.

^{1}H NMR (300 MHz, $CDCl_3$): δ (ppm) = 4.82 (sept, J = 7.1 Hz, 2 H, NCH), 2.33 (s, 6 H, CCH_3), 1.63 (d, J = 7.0 Hz, 12 H, CH(CH_3)$_2$).

^{11}B{^{1}H} NMR (96 MHz, $CDCl_3$): δ (ppm) = -1.07.

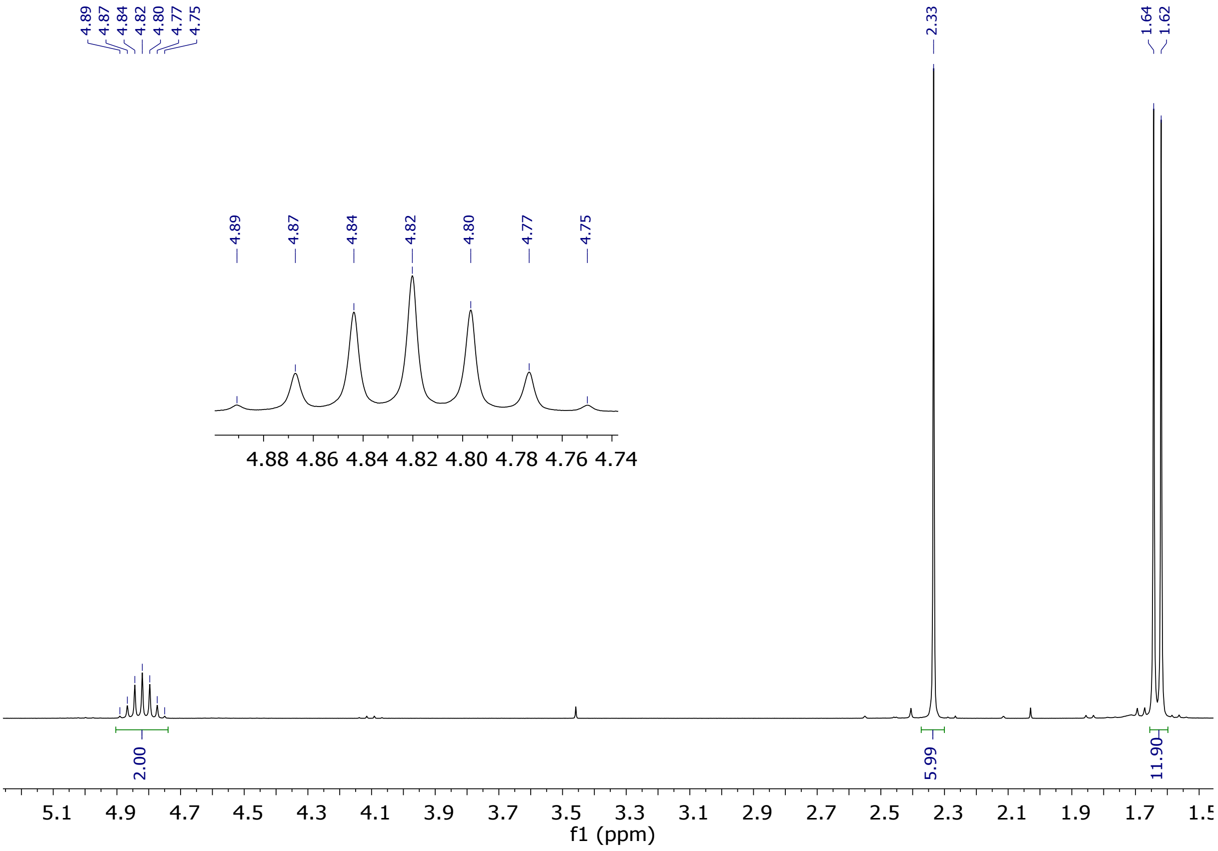

Figure S3: ^{1}H NMR spectrum of compound **3**, (300 MHz, $CDCl_3$, 25 °C).

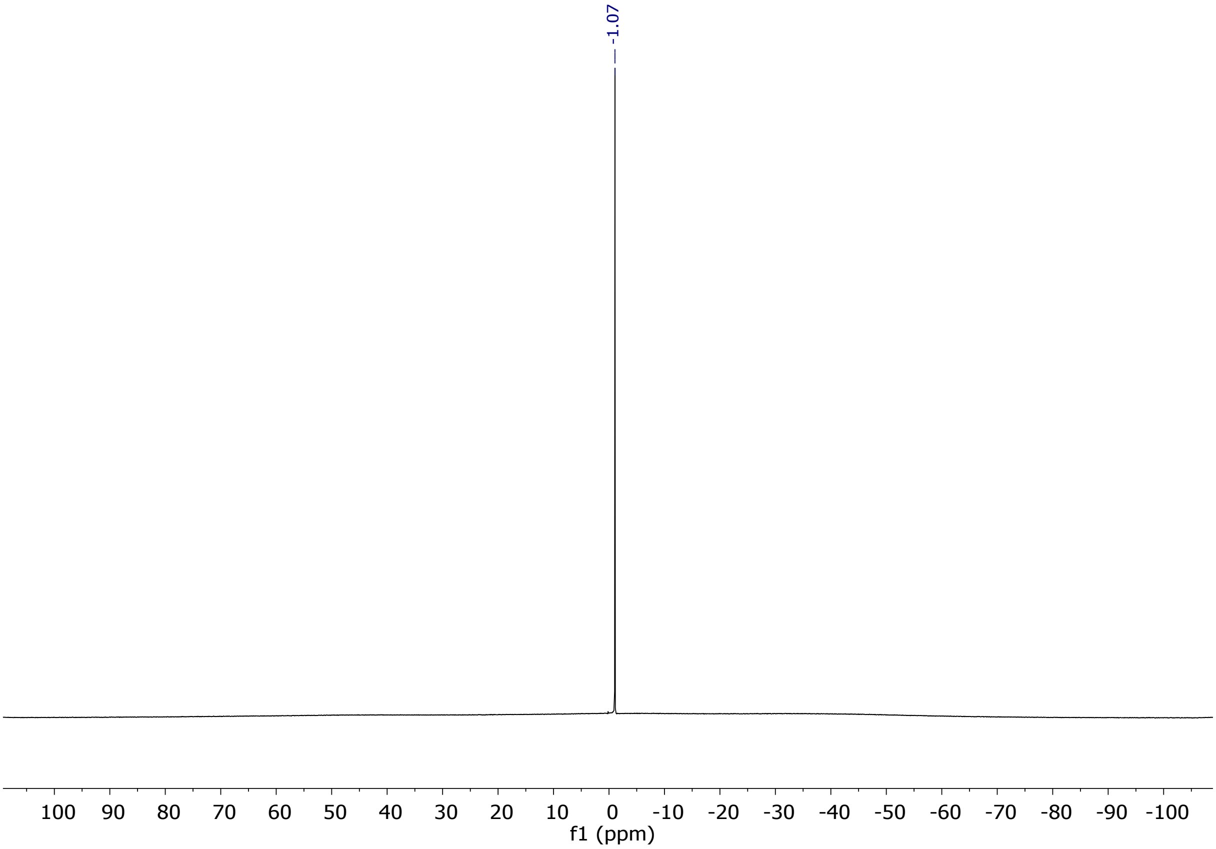

Figure S4: ${}^{11}B\{{}^{1}H\}$ NMR spectrum of compound **3**, (96 MHz, $CDCl_3$, 25 °C).

2.3 2,6-Diisopropyl-*N*-(2-{1,3-Diisopropyl-4,5-dimethyl-4-imidazoline-2-iminyl}phenyl)-aniline

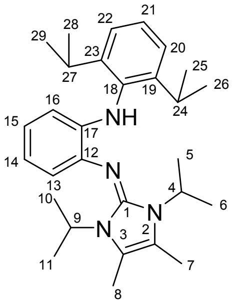

HAmIm

1

Method A:

Amine **2** (3.26 g, 12.1 mmol, 1.0 eq.) and imidazolium salt **3** (4.08 g, 13.5 mmol, 1.1 eq.) were dissolved in MeCN (100 mL). CsF (12.3 g, 81 mmol, 6.0 eq.) was added to the solution and the reaction mixture was stirred for 24 h at 65 °C. The reaction mixture was stored at -20 °C for 18 h to complete the precipitation of the product. After filtration in air the remaining CsF was removed from crude product by extraction with $CHCl_3$ (100 mL) and the organic solution was washed with water (50 mL). The organic layer was separated, dried over Mg_2SO_4 and dried under reduced pressure. The solid residue was recrystallized from hot MeCN to afford product **1** (2.24 g, 5.02 mmol, 42 %) as beige powder.

Method B:

Amine **2** (0.76 g, 2.84 mmol, 1.0 eq.) and imidazolium salt **3** (1.0g, 3.31 mmol, 1.1 eq.) were dissolved in MeCN (60 mL). CsF (2.87 g, 18.9 mmol, 6.7 eq.) was added to the solution and the reaction mixture was stirred for 24 h at 65 °C. The solution was filtered and solvent was removed *in vacuo*. The residue was washed with Et_2O (20 mL) to afford a colourless crystalline solid. The solid was dissolved in MeOH (5 mL). Hexane (25 mL) and 50% aqueous KOH solution was added and stirred vigorously for 1 h at 25 °C. The hexane layer was separated and the remaining mixture was extracted with hexane (2 × 25 mL). The organic layers were combined, dried over $MgSO_4$ and the solvent was reduced. The crude product was crystallized from hot MeCN to obtain product **1** (507 mg, 1.14 mmol, 40%) as beige solid.

^{1}H NMR (400 MHz, $CDCl_3$): δ (ppm) = 7.33 – 7.22 (m, 3 H, aryl C−*H* in Dipp), 6.62 – 6.53 (m, 2 H, C13−*H*, C14−*H*), 6.49 (ddd, *J* = 7.6, 6.0, 2.9 Hz, 1 H, C15−*H*), 6.45 (br, 1 H, N4*H*), 6.14 – 6.06 (m, 1 H, C16−*H*), 4.64 (sept, *J* = 7.0 Hz, 2 H, NC*H*$(CH_3)_2$), 3.35 (sept, *J* = 6.9 Hz, 2 H, C*H*$(CH_3)_2$), 2.17 (s, 6 H, backbone CH_3), 1.42 (d, *J* = 7.0 Hz, 12 H, NCH(CH_3)$_2$), 1.21 (d, *J* = 6.9 Hz, 12 H, CH(CH_3)$_2$).

^{13}C{^{1}H} NMR (100 MHz, $CDCl_3$): δ (ppm) = 149.7 (s, *C*1), 147.6 (s, *C*19, *C*23), 140.1 (s, *C*12), 139.3 (s, *C*17), 138.1 (s, *C*18), 126.2 (s, *C*21), 123.5 (s, *C*20, *C*22), 117.2 (s, *C*2, *C*3), 116.8 (s, *C*14), 116.8 (s, *C*15), 114.6 (s, *C*13), 109.6 (s, *C*16), 46.6 (s, *C*4, *C*9), 28.4 (s, *C*24, *C*27), 25.1, 23.2 (both br, *C*25, *C*26, *C*28, *C*29), 21.1 (s, *C*5, *C*6, *C*10, *C*11), 10.5 (s, *C*7, *C*8).

Elemental Analysis. Calcd. for $C_{29}H_{42}N_4$: C 77.98, H 9.48, N 12.54. Found: C 77.24, H 9.66, N 12.22.

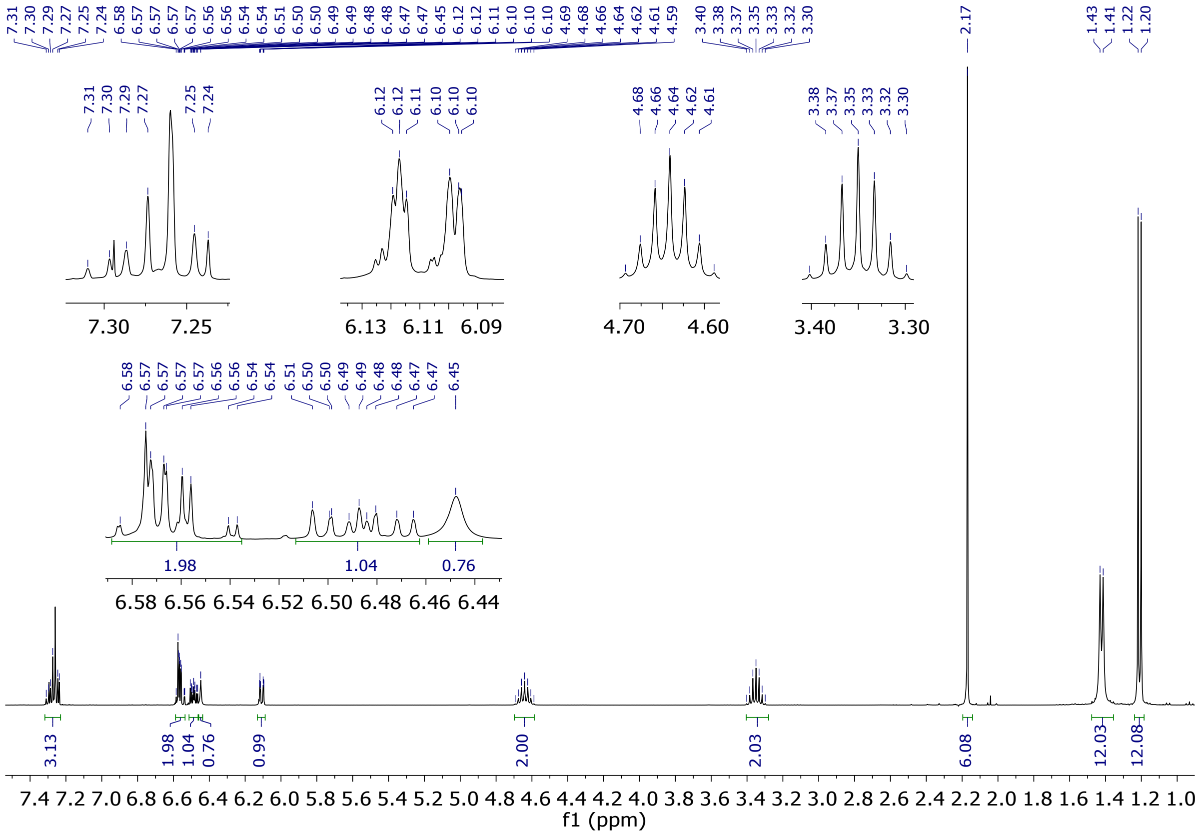

Figure S5: ^{1}H NMR spectrum of compound **1**, (400 MHz, $CDCl_3$, 25 °C).

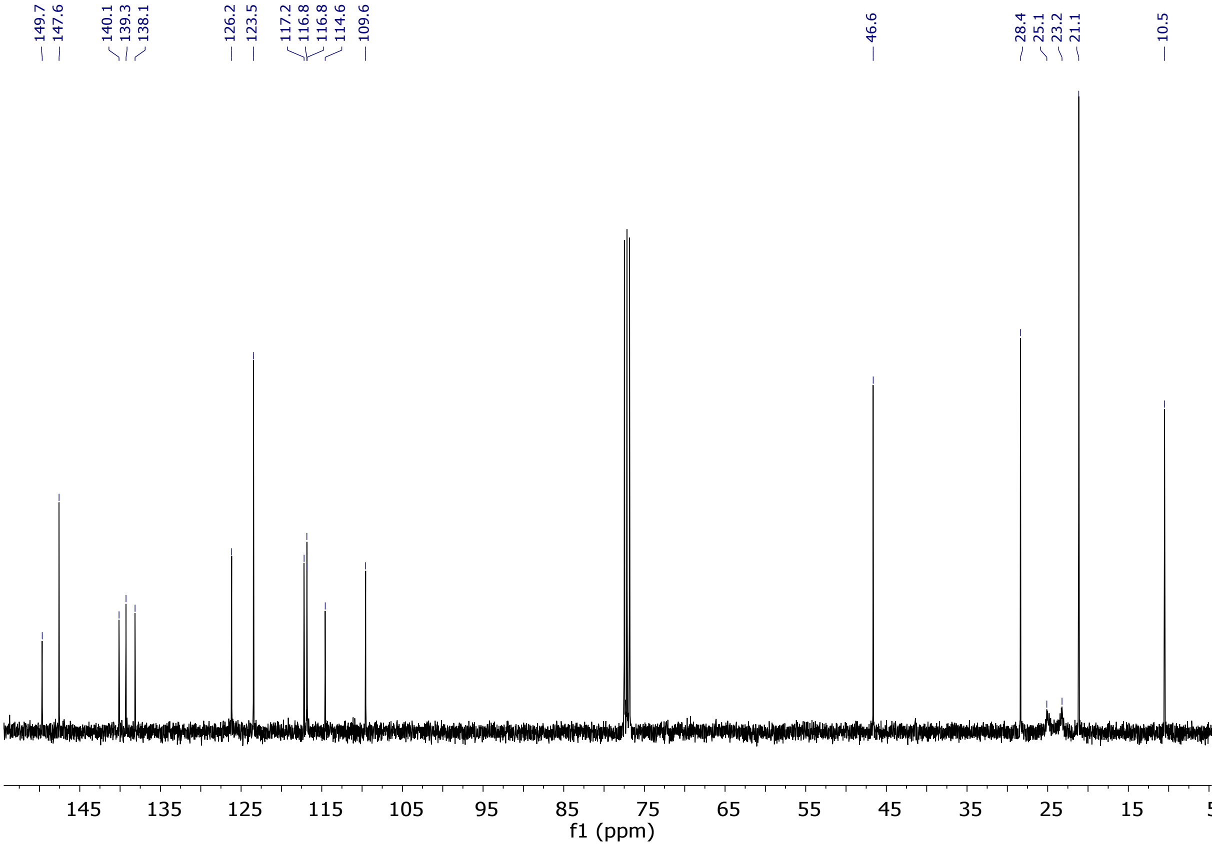

Figure S6: $^{13}C\{^{1}H\}$ NMR spectrum of compound **1**, (100 MHz, C_6D_6, 25 °C).

2.4 Ga(AmIm) **4**

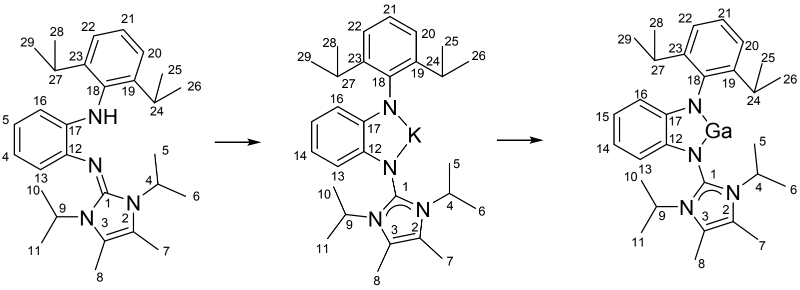

HAmIm **1** K(AmIm) Ga(AmIm) **4**

K(AmIm): HAmIm **1** (500 mg, 1.12 mmol, 1.0 eq.) was dissolved in toluene (5 mL) and a suspension of benzyl potassium KBn (175 mg, 1.34 mmol, 1.2 eq.) in toluene (5 mL) was added at 25 °C. The deep red color of solid KBn faded to a yellowish appearance with significant dissolution. After stirring for 1 h *n*-hexane (15 mL) was added and the precipitate was allowed to settle at the bottom of the flask. The supernatant solution was decanted and the solid product was dried *in vacuo* to give the product K(AmIm) (430 mg, 0.89 mmol, 79 %) as a yellowish powder.

^{1}H NMR (300 MHz, THF-D$_8$): δ (ppm) = 6.89 (d, J = 7.5 Hz, 2 H, C20−*H*, C22−*H*), 6.59 (t, J = 7.5 Hz, 1 H, C21−*H*), 6.15 (ddd, J = 7.9, 7.0, 1.8 Hz, 1 H, C14−*H*), 6.09 (dd, J = 7.2, 1.8 Hz, 1 H, C16−*H*), 5.55 (td, J = 7.1, 1.5 Hz, 1 H, C15−*H*), 5.41 (dd, J = 7.9, 1.5 Hz, 1 H, C13−*H*), 4.80 (sept, J = 7.1 Hz, 2 H, NC*H*(CH$_3$)$_2$), 3.66 – 3.47 (m, 2 H, C*H*(CH$_3$)$_2$), 2.09 (s, 6 H, C*H*$_3$), 1.30 (d, J = 7.1 Hz, 6 H, NCH(C*H*$_3$)$_2$), 1.21 (d, J = 7.0 Hz, 6 H, NCH(C*H*$_3$)$_2$), 1.04 (dd, J = 6.9, 1.5 Hz, 12 H, CH(C*H*$_3$)$_2$).

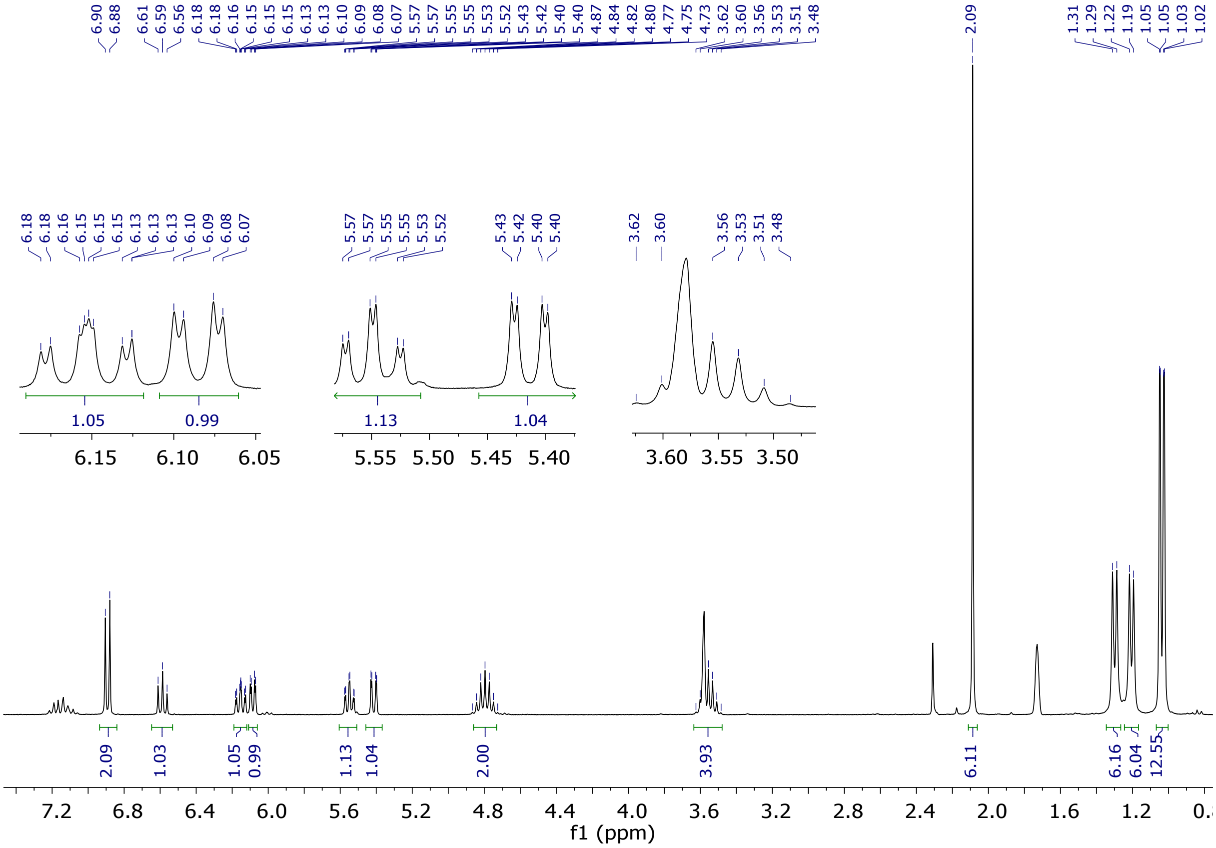

Figure S7: ^{1}H NMR spectrum of compound K(AmIm), (300 MHz, THF-D$_8$, 25 °C).

Ga(AmIm) **4**: Potassium salt K(AmIm) (200 mg, 0.42 mmol, 1.0 eq.) was dissolved in THF (10 mL) and GaCp* (95 mg, 0.42 mmol, 1.0 eq.) was added to the solution. The reaction was stirred for 30 min at 25 °C, during which a precipitate formed. The solid was removed by filtration and the resulting solution was reduced to 4 mL and *n*-pentane (20 mL) was added. The solution was stored at −40 °C to afford product **4** (144 mg, 0.3 mmol, 67 %) as yellowish crystals suitable for X-ray crystallography.

^{1}H NMR (400 MHz, C_6D_6): δ (ppm) = 7.46(m, 2 H, C20−*H*, C22−*H*), 7.37 (dd, *J* = 8.4, 6.8 Hz, 1 H, C21−*H*), 6.87 (ddd, *J* = 7.8, 7.3, 1.4 Hz, 1 H, C14−*H*), 6.64 (td, *J* = 7.3, 1.4 Hz, 1 H, C15−*H*), 6.44 (dd, *J* = 7.8, 1.4 Hz, 1 H, C16−*H*), 6.10 (dd, *J* = 7.5, 1.4 Hz, 1 H, C13−*H*), 4.53 (sept, *J* = 7.1 Hz, 2 H, NC*H*$(CH_3)_2$), 3.67 (sept, *J* = 6.9 Hz, 2 H, C*H*$(CH_3)_2$), 1.50 (d, *J* = 6.7 Hz, 12 H, CH_3 and CH(CH_3)$_2$), 1.29 (d, *J* = 6.9 Hz, 6 H, CH(CH_3)$_2$), 1.11 (d, *J* = 7.1 Hz, 6 H, NCH(CH_3)$_2$), 0.93 (d, *J* = 7.2 Hz, 6 H, NCH(CH_3)$_2$).

^{13}C{^{1}H} NMR (100 MHz, C_6D_6): δ (ppm) = 150.4 (s, *C*1), 148.5 (s, *C*12), 146.6 (s, *C*19, *C*23), 144.4 (s, *C*18), 141.5 (s, *C*17), 124.8 (s, *C*21), 123.7 (s, *C*20, *C*22), 120.7 (s, *C*2, *C*3), 119.4 (s, *C*14), 112.9 (s, *C*15), 111.2 (s, *C*13), 110.7 (s, *C*16), 48.7 (s, N*C*H$(CH_3)_2$), 28.7 (s, *C*H$(CH_3)_2$), 26.8 (s, CH(*C*H$_3$)$_2$), 24.5 (s, CH(*C*H$_3$)$_2$), 22.3 (s, NCH(*C*H$_3$)$_2$), 21.3 (s, NCH(*C*H$_3$)$_2$), 9.6 (s, *C*7, *C*8).

Elemental Analysis. Calcd. for $C_{29}H_{41}N_4Ga$: C 67.58, H 8.02, N 10.87. Found: C 66.35, H 8.02, N 11.37. The value for carbon is by 1.25 % lower than expected despite the use of V2O5 as a combustion agent. We expect the formation of GaC to be the reason for the deviation observed.

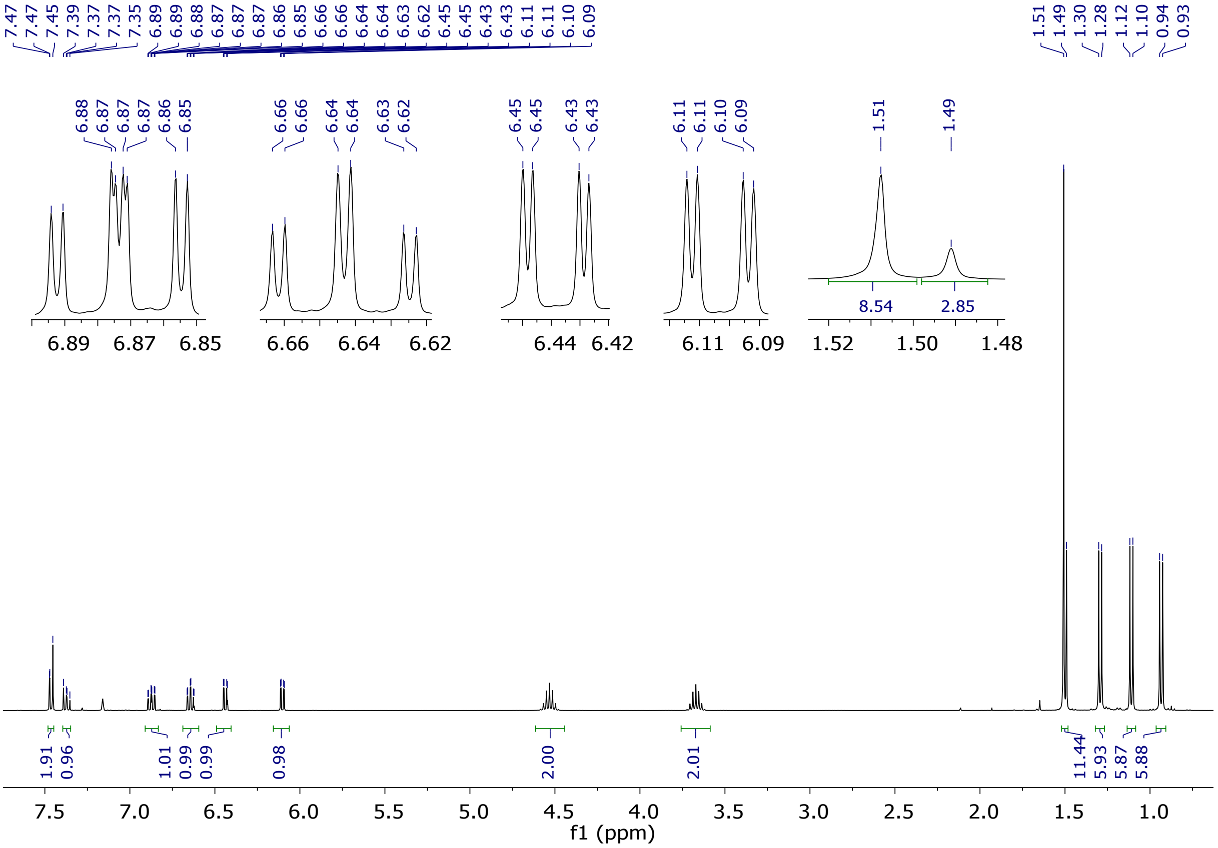

Figure S8: ^{1}H NMR spectrum of compound **4**, (400 MHz, C_6D_6, 25 °C).

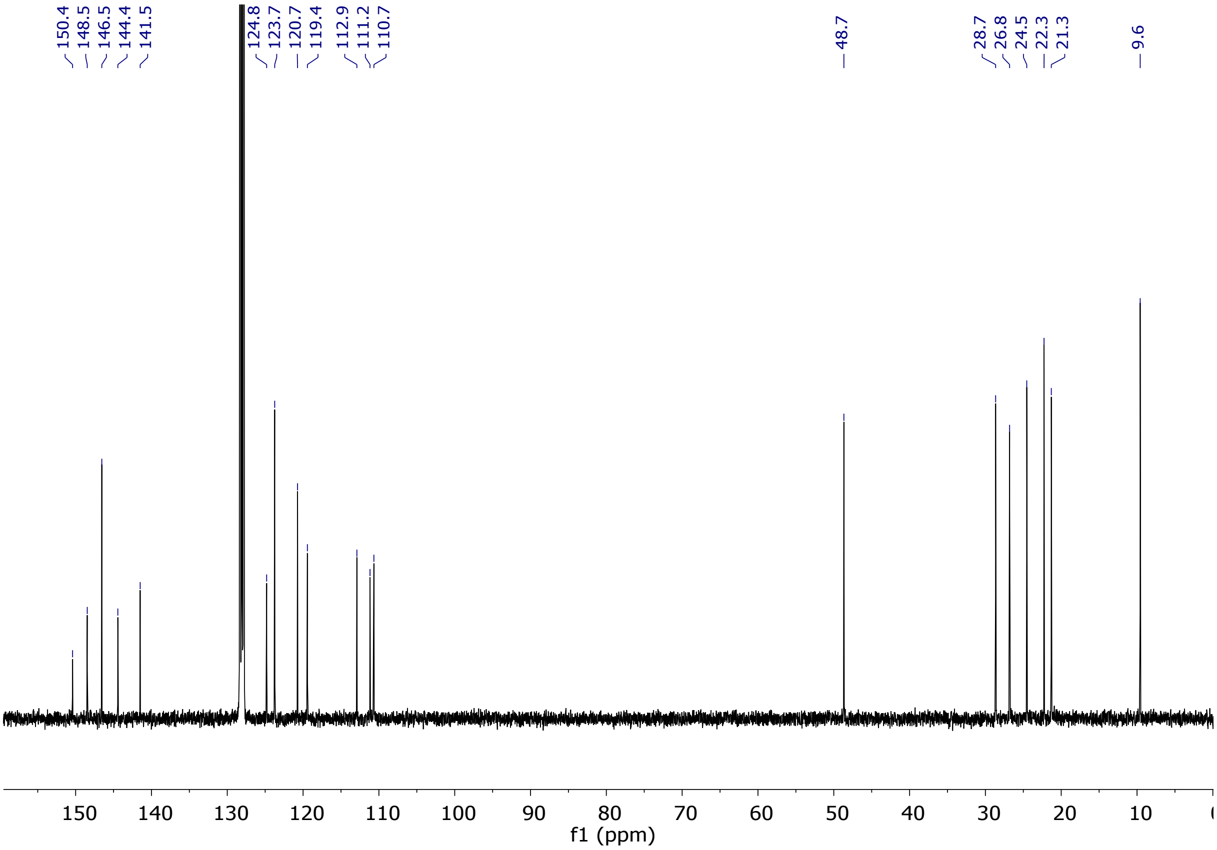

Figure S9: $^{13}C\{^{1}H\}$ NMR spectrum of compound **4**, (100 MHz, C_6D_6, 25 °C).

2.5 In(AmIm) **5**

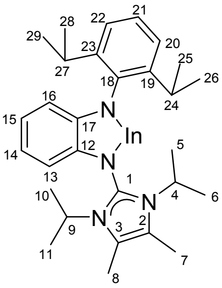

In(AmIm)

5

HAmIm **1** (150 mg, 0.34 mmol, 1.0 eq.) was dissolved in THF (5 mL) and *n*-BuLi (1.6 M in *n*-hexane, 0.7 mL, 1.12 mmol, 1.0 eq.) was added at 25 °C. The solution was stirred for 30 min and InCp (73.0 mg, 0.4 mmol, 1.2 eq.) dissolved in THF (5 mL) was added. The solution turned dark yellow and a grey precipitate was formed. After stirring for 1 h the solvent was removed *in vacuo*. The residue was extracted with toluene (25 mL) and filtered over Celite®. The filtrate was reduced to 2 mL and *n*-pentane (50 mL) was added. The solution was stored at −40 °C to afford the product **5** (65 mg, 0.12 mmol, 35 %) as orange crystals suitable for X-ray crystallography.

^{1}H NMR (400 MHz, C_6D_6): δ (ppm) = 7.50 – 7.45 (m, 2 H, C20−*H*, C22−*H*), 7.35 (dd, *J* = 8.2, 7.0 Hz, 1 H, C21−*H*), 6.86 (ddd, *J* = 7.9, 7.2, 1.5 Hz, 1 H, C14−*H*), 6.58 (td, *J* = 7.3, 1.5 Hz, 1 H, C15−*H*), 6.39 (dd, *J* = 7.9, 1.4 Hz, 1 H, C16−*H*), 6.12 (dd, *J* = 7.5, 1.5 Hz, 1 H, C13−*H*), 4.57 (sept, *J* = 7.1 Hz, 2 H, $NC\mathit{H}(CH_3)_2$), 3.72 (sept, *J* = 6.9 Hz, 2 H, $C\mathit{H}(CH_3)_2$), 1.50 (s, 6 H, $C\mathit{H}_3$), 1.46 (d, *J* = 7.0 Hz, 6 H, $CH(C\mathit{H}_3)_2$), 1.30 (d, *J* = 6.9 Hz, 6 H, $CH(C\mathit{H}_3)_2$), 1.07 (d, *J* = 7.1 Hz, 6 H, $NCH(C\mathit{H}_3)_2$), 0.93 (d, *J* = 7.1 Hz, 6 H, $NCH(C\mathit{H}_3)_2$).

^{13}C{^{1}H} NMR (100 MHz, C_6D_6): δ (ppm) = 151.8 (s, *C*1), 150.6 (s, *C*12), 146.7 (s, *C*18), 145.9 (s, *C*19 *C*23), 142.4 (s, *C*17), 124.1 (s, *C*21), 123.8 (s, *C*20, *C*22), 119.9 (s, *C*14), 119.8 (s, *C*2, *C*3), 113.7 (s, *C*13), 112.0(s, *C*15), 111.9(s, *C*16), 48.1 (s, $N\mathit{C}H(CH_3)_2$), 28.4 (s, $\mathit{C}H(CH_3)_2$), 27.0 (s, $CH(\mathit{C}H_3)_2$), 24.7 (s, $CH(\mathit{C}H_3)_2$), 22.4(s, $NCH(\mathit{C}H_3)_2$), 21.2 (s, $NCH(\mathit{C}H_3)_2$), 9.6 (s, *C*7, *C*8).

Elemental Analysis. Calcd. for $C_{29}H_{41}N_4In$: C 62.15, H 7.37, N 10.0. Found: C 62.15, H 7.73, N 9.39.

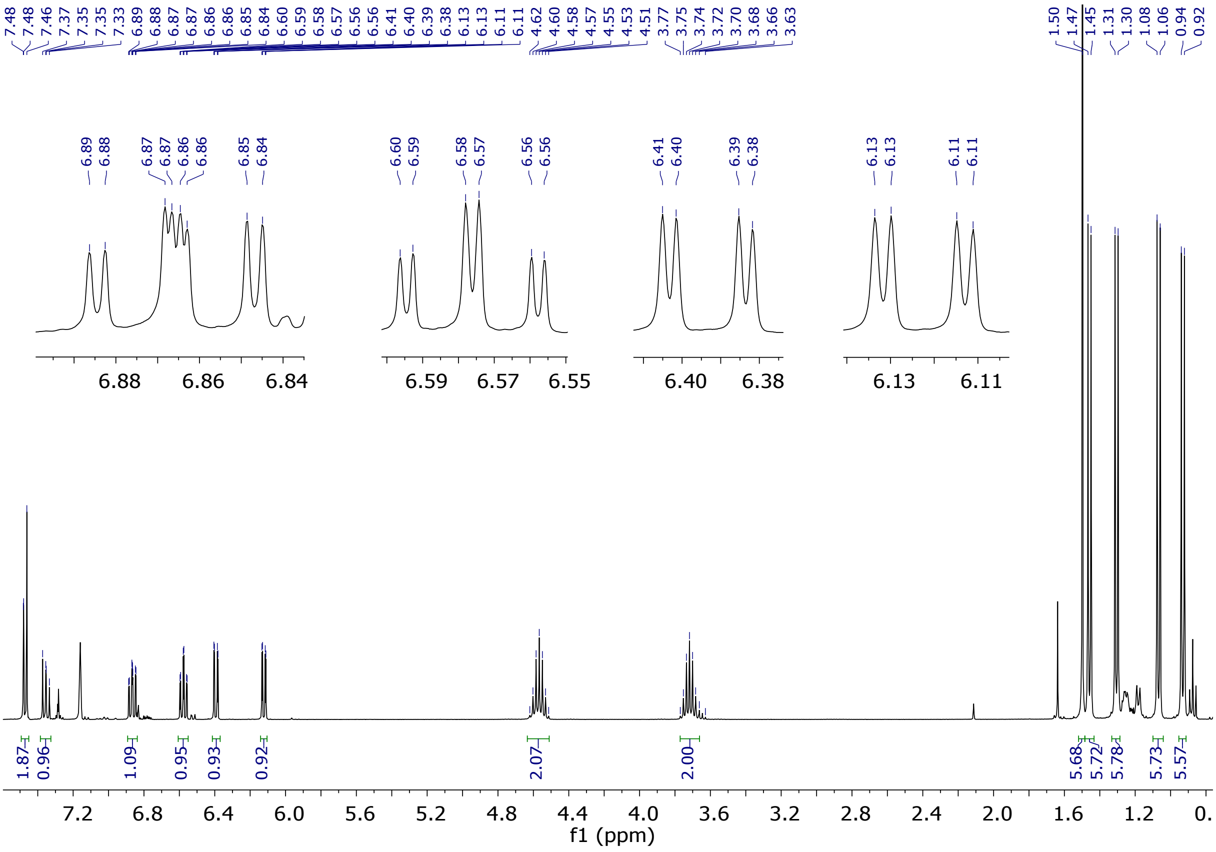

Figure S10: ^{1}H NMR spectrum of compound **5**, (400 MHz, C_6D_6, 25 °C).

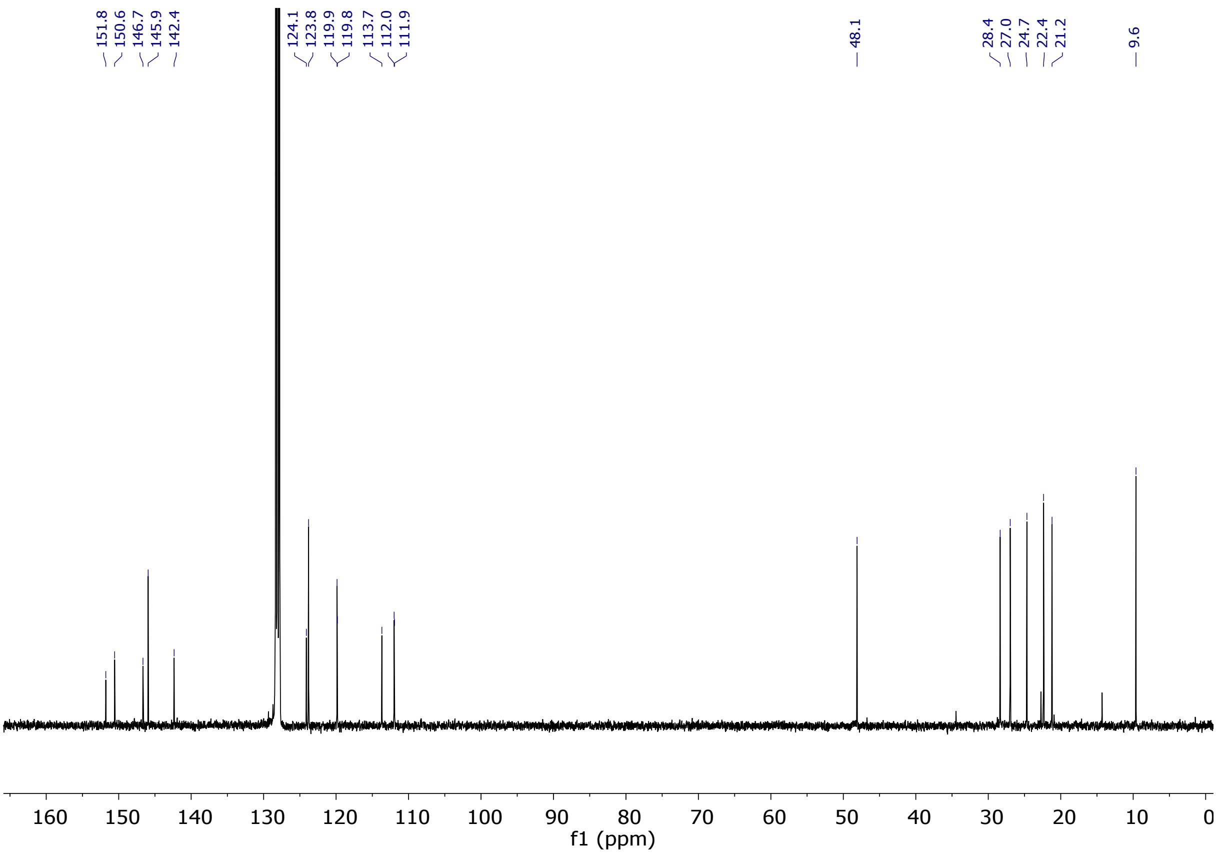

Figure S11: $^{13}C\{^1H\}$ NMR spectrum of compound **5**, (100 MHz, C_6D_6, 25 °C).

2.6 Tl(AmIm) 6

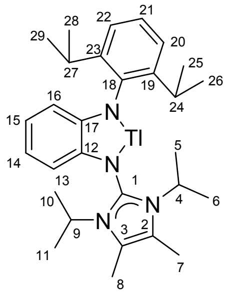

Tl(AmIm)

6

HAmIm **1** (500 mg, 1.12 mmol, 1.0 eq.) was dissolved in THF (10 mL). *n*-BuLi (1.6 M in *n*-hexane, 0.7 mL, 1.12 mmol, 1.0 eq.) was added to the solution at 25 °C and the reaction mixture was stirred for 30 min. $TlBF_4$ (320 mg, 1.12 mmol, 1.0 eq.) was dissolved in THF (4 mL) and added to the reaction. After stirring for 24 h, the solvent was evaporated and the residue was dissolved in toluene (35 mL). The dark red solution was filtered over Celite®. The solution was reduced to 10 mL and layered with *n*-hexane (25 mL), which afforded product **6** (305 mg, 0.47 mmol, 43 %) as dark red crystals suitable for X-ray crystallography.

^{1}H NMR (400 MHz, C_6D_6): δ (ppm) = 7.51 (d, J = 7.6 Hz, 2 H, C20−*H*, C22−*H*), 7.30 (t, J = 7.6 Hz, 1 H, C21−*H*), 6.92 – 6.82 (m, 1 H, C14−*H*), 6.48 (td, J = 7.3, 1.5 Hz, 1 H C15−*H*), 6.26 (dd, J = 7.5, 1.6 Hz, 1 H, C16−*H*), 6.21 (d, J = 7.9 Hz, 1 H, C13−*H*), 4.58 (sept, J = 7.1 Hz, 2 H, $NCH(CH_3)_2$), 3.73 (sept, J = 6.9 Hz, 2 H, $CH(CH_3)_2$), 1.56 (s, 6 H, CH_3), 1.40 (d, J = 7.0 Hz, 6 H, $CH(CH_3)_2$), 1.31 (d, J = 7.0 Hz, 6 H, $CH(CH_3)_2$), 1.04 (d, J = 7.1 Hz, 6 H, $NCH(CH_3)_2$), 0.99 (d, J = 7.1 Hz, 6 H, $NCH(CH_3)_2$).

$^{13}C\{^1H\}$ NMR (100 MHz, C_6D_6): δ (ppm) = 155.2(s, *C*12), 153.1(s, *C*1), 148.8 (s, *C*18), 145.9 (s, *C*19, *C*23), 144.8 (s, *C*17), 123.7 (s, *C*20, *C*22), 123.6 (s, *C*21), 120.5 (s, *C*14), 118.9 (s, *C*16), 117.6 (s, *C*2, *C*3), 114.8 (s, *C*13), 111.8 (s, *C*15), 47.4 (s, N*C*H(CH_3)$_2$), 27.8 (s, *C*H(CH_3)$_2$), 27.5 (br, CH(CH_3)$_2$), 24.8 (s, CH(CH_3)$_2$), 22.5 (br, NCH(CH_3)$_2$), 21.2 (s, NCH(CH_3)$_2$), 9.7 (s, *C*7, *C*8).

Elemental Analysis. Calcd. for $C_{29}H_{41}N_4Tl$: C 53.58, H 6.36, N 8.62. Found: C 53.74, H 6.59, N 8.44.

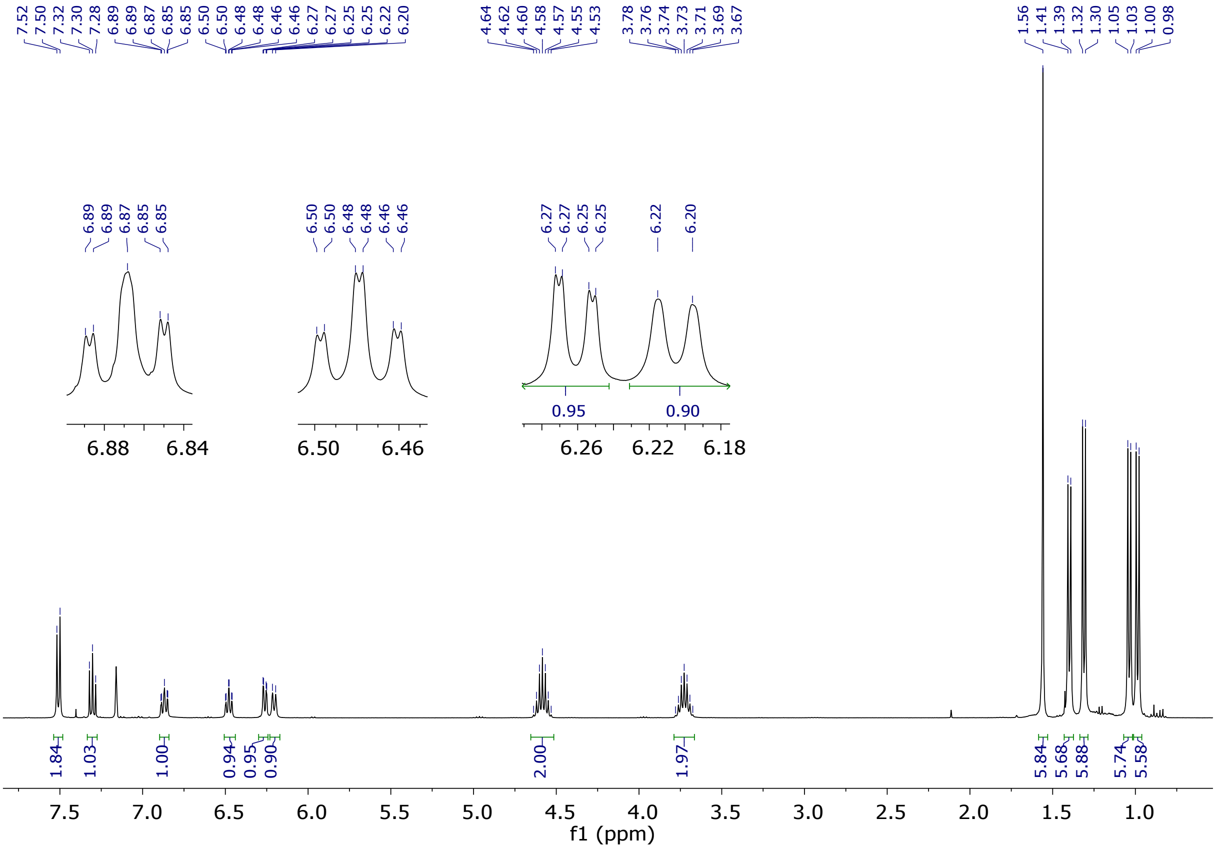

Figure S12: ^1H NMR spectrum of compound **6**, (400 MHz, C_6D_6, 25 °C).

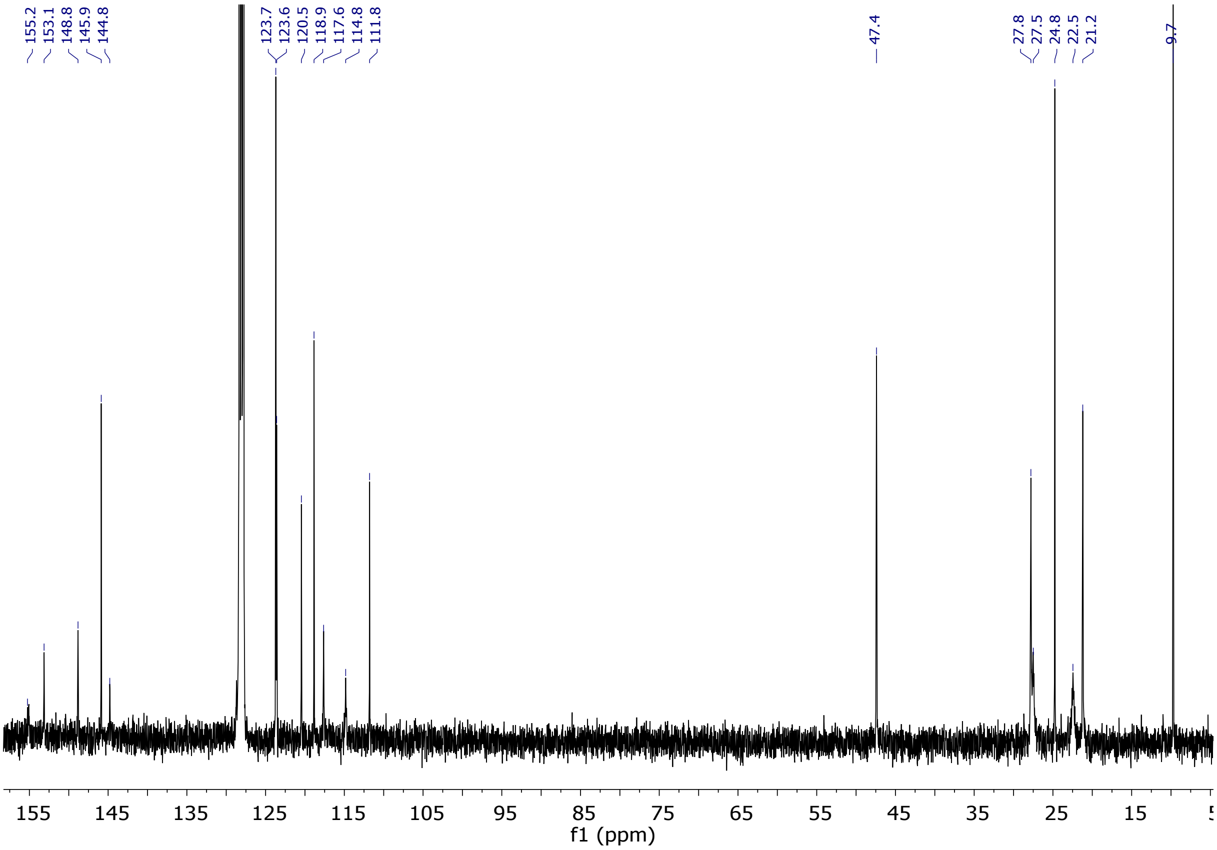

Figure S13: $^{13}C\{^{1}H\}$ NMR spectrum of compound **6**, (100 MHz, C_6D_6, 25 °C).

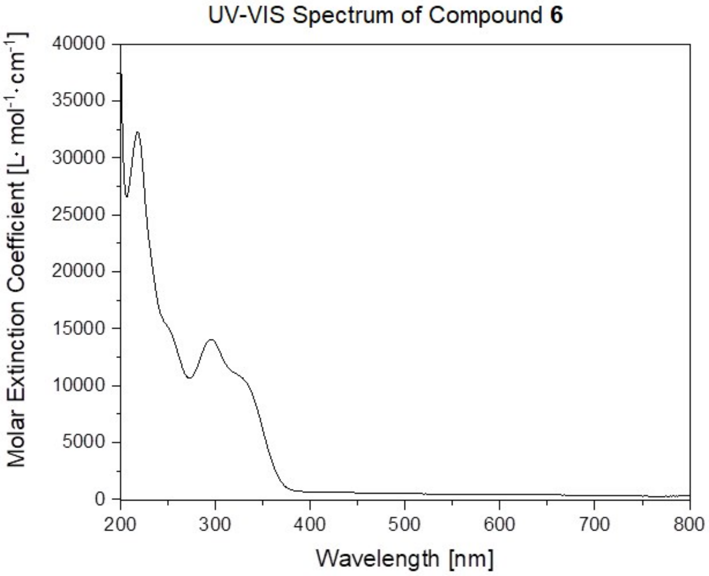

Figure S14: UV-VIS spectrum of compound **6** in n-hexane, 25 °C.

2.7 [Fe(CO)$_4${Ga(AmIm)}] **7**

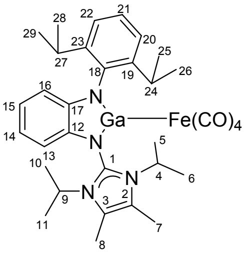

[Fe(CO)$_4${Ga(AmIm)}]

7

Ga(I) carbenoide **4** (50 mg, 0.097 mmol, 1.0 eq.) was dissolved in toluene (5 mL) and treated with an excess of iron pentacarbonyl (26.2 µL, 0.194 mmol, 2.0 eq.). The reaction mixture was stirred at 25 °C for 18 h. The solvent was removed *in vacuo* to afford an off-white solid. Crystallization of the solid from toluene at −40 °C gave product **7** (65 mg, 0.095 mmol, 98 %) as colourless crystals suitable for X-ray crystallography.

^{1}H NMR (600 MHz, C$_6$D$_6$): *δ* (ppm) = 7.38 – 7.31 (m, 3 H, C20−*H*, C21−*H*, C22−*H*), 6.81 (ddd, *J* = 7.9, 7.4, 1.4 Hz, 1 H, C14−*H*), 6.62 (td, *J* = 7.5, 1.4 Hz, 1 H, C15−*H*), 6.49 (dd, *J* = 7.9, 1.3 Hz, 1 H, C16−*H*), 5.92 (dd, *J* = 7.7, 1.4 Hz, 1 H, C13−*H*), 4.47 (sept, *J* = 7.1 Hz, 2 H, NC*H*(CH$_3$)$_2$), 3.55 (sept, *J* = 6.9 Hz, 2 H, C*H*(CH$_3$)$_2$), 1.52 (d, *J* = 6.9 Hz, 6 H, CH(C*H*$_3$)$_2$), 1.49 (s, 6 H, C*H*$_3$), 1.25 (d, *J* = 7.1 Hz, 6 H, NCH(C*H*$_3$)$_2$), 1.17 (d, *J* = 6.9 Hz, 6 H, CH(C*H*$_3$)$_2$), 0.82 (d, *J* = 7.0 Hz, 6 H, NCH(C*H*$_3$)$_2$).

^{13}C{^{1}H} NMR (150 MHz, C$_6$D$_6$): *δ* (ppm) = 216.6 (s, *C*O), 146.5 (s, *C*19, *C*23), 145.3 (s, *C*1), 145.0 (s, *C*12), 140.3 (s, *C*18), 138.9 (s, *C*17), 127.0 (s, *C*21), 124.3 (s, *C*20, *C*22), 123.0 (s, *C*2, *C*3), 121.0 (s, *C*14), 115.5 (s, *C*15), 111.5 (s, *C*16), 110.9 (s, *C*13), 49.9 (s, N*C*H(CH$_3$)$_2$), 29.1 (s, *C*H(CH$_3$)$_2$), 24.9 (s, CH(*C*H$_3$)$_2$), 24.9 (s, CH(*C*H$_3$)$_2$, 21.2(s, NCH(*C*H$_3$)$_2$), 20.8 (s, NCH(*C*H$_3$)$_2$), 9.4 (s, *C*7, *C*8).

Elemental Analysis. Calcd. for C$_{33}$H$_{41}$N$_4$O$_4$GaFe: C 57.37, H 6.00, N 8.12. Found: C 56.77, H 6.05, N 7.90.

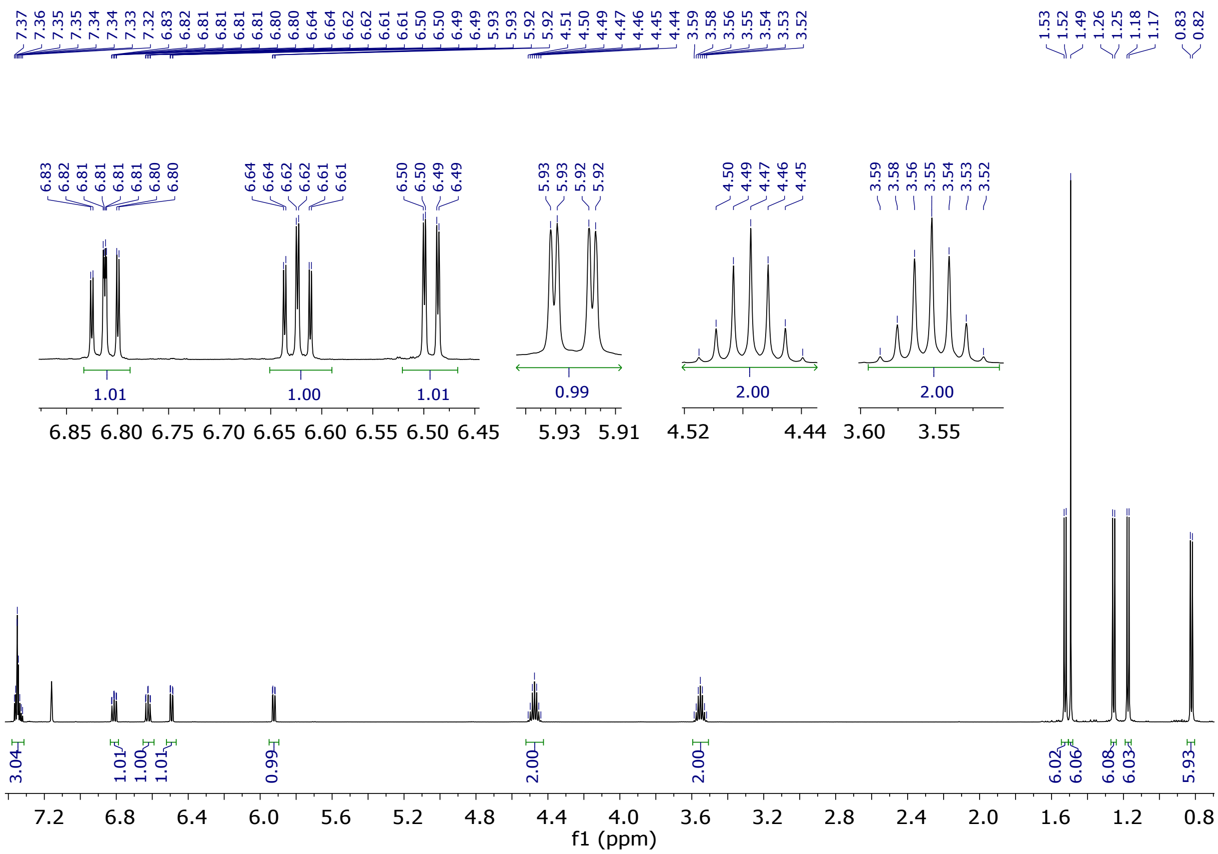

Figure S15: ^{1}H NMR spectrum of compound **7**, (600 MHz, C_6D_6, 25 °C).

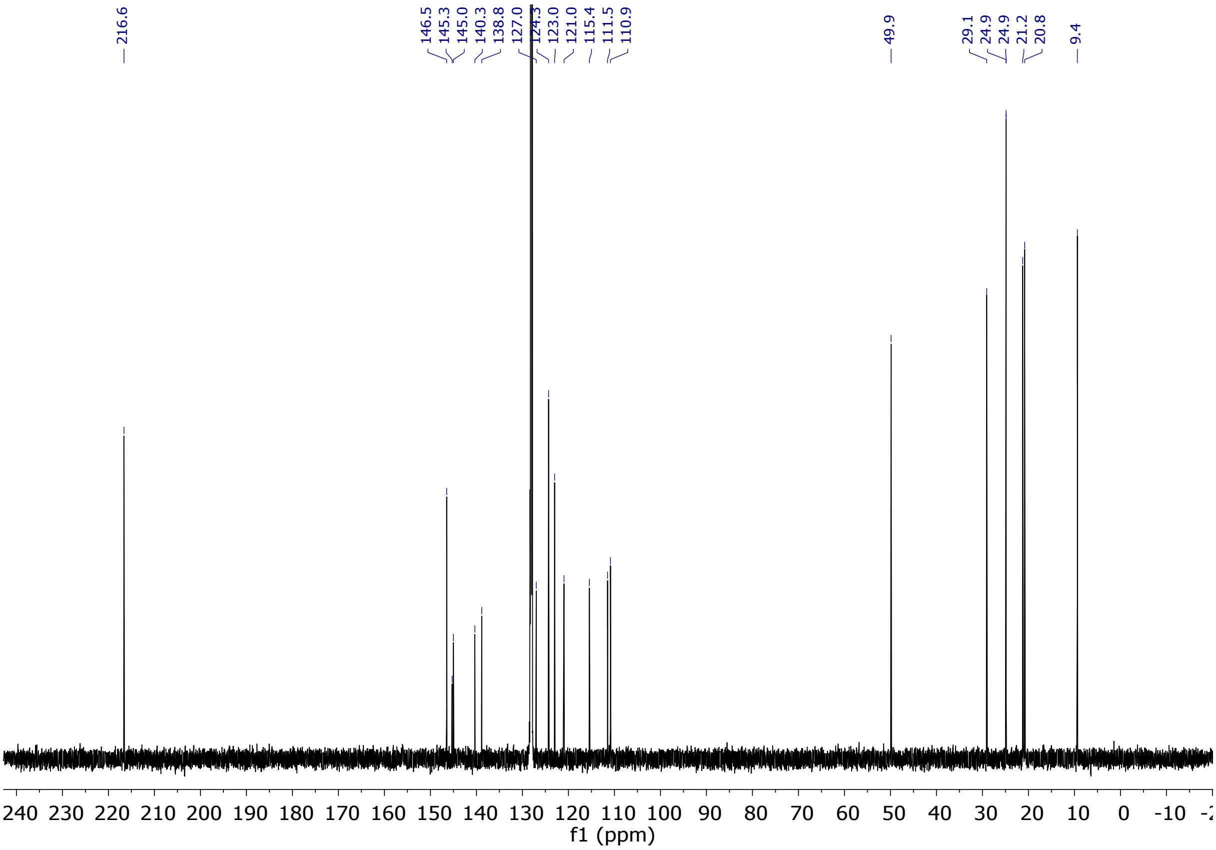

Figure S16: $^{13}C\{^{1}H\}$ NMR spectrum of compound **7**, (150 MHz, C_6D_6, 25 °C).

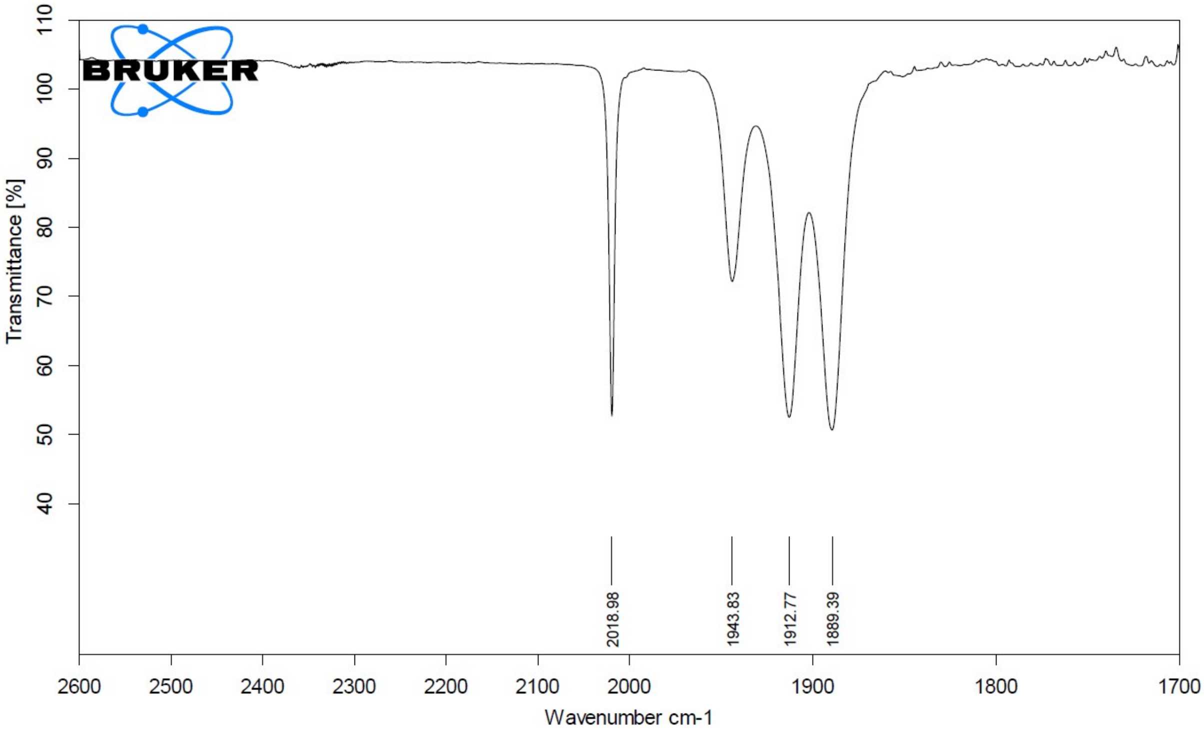

Figure S17: FT-IR spectrum of compound **7** in toluene.

2.8 [W(CO)$_5${Ga(AmIm)}] **8**

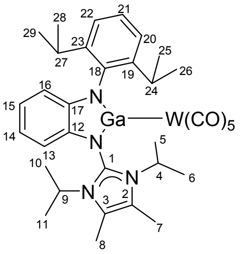

[W(CO)$_5${Ga(AmIm)}]

8

Ga(I) carbenoide **4** (50 mg, 0.097 mmol, 1.0 eq.) and W(CO)$_5$NMe$_3$ (50 mg, 0.097 mmol, 1.0 eq.) were dissolved in toluene (5 mL) The yellowish reaction mixture was stirred at 25 °C for 18 h. After pale the mixture was freed from the solvent *in vacuo* to afford an off-white solid. Crystallization of the solid from toluene at −40 °C gave product **8** (70 mg, 0.084 mmol, 86 %) as colourless crystals suitable for X-ray crystallography.

^{1}H NMR (600 MHz, C$_6$D$_6$): δ (ppm) = 7.39 – 7.32 (m, 3 H, C20−*H*, C21−*H*, C22−*H*), 6.82 (ddd, *J* = 7.9, 7.4, 1.4 Hz, 1 H, C14−*H*), 6.63 (td, *J* = 7.5, 1.4 Hz, 1 H, C15−*H*), 6.48 (dd, *J* = 7.9, 1.3 Hz, 1 H, C16−*H*), 5.87 (dd, *J* = 7.6, 1.3 Hz, 1 H, C13−*H*), 4.38 (sept, *J* = 7.1 Hz, 2 H, NC*H*(CH$_3$)$_2$), 3.54 (sept, *J* = 7.0 Hz, 2 H, C*H*(CH$_3$)$_2$), 1.54 (d, *J* = 6.9 Hz, 6 H, CH(C*H*$_3$)$_2$), 1.51 (s, 6 H, C*H*$_3$), 1.21 (d, *J* = 7.1 Hz, 6 H, NCH(C*H*$_3$)$_2$), 1.19 (d, *J* = 6.9 Hz, 6 H, CH(C*H*$_3$)$_2$), 0.85 (d, *J* = 7.1 Hz, 6 H, NCH(C*H*$_3$)$_2$).

^{13}C{^{1}H} NMR (150 MHz, C$_6$D$_6$): δ (ppm) = 203.4 ($^1J_{\text{CW}}$ = 79 Hz, *C*O$_{\text{ax}}$), 200.3 ($^1J_{\text{CW}}$ = 60.2 Hz, *C*O$_{\text{eq}}$), 146.4 (s, *C*19, *C*23), 146.1 (s, *C*1), 145.7 (s, *C*12), 140.8 (s, *C*18), 139. 9 (s, *C*17), 126.67 (s, *C*21), 124.2 (s, *C*20, *C*22), 122.9 (s, *C*2, *C*3), 120.4 (s, *C*14), 114.9 (s, *C*15), 110.9 (s *C*16), 110.1 (s, *C*13), 49.7 (s, N*C*H(CH$_3$)$_2$), 29.1 (s, *C*H(CH$_3$)$_2$), 25.4 (s, CH(*C*H$_3$)$_2$), 24.6 (s, CH(*C*H$_3$)$_2$), 21.5 (s, NCH(*C*H$_3$)$_2$), 21.4 (s, NCH(*C*H$_3$)$_2$), 9.3 (s, *C*7, *C*8).

Elemental Analysis. Calcd. for C$_{34}$H$_{41}$N$_4$O$_5$GaW: C 48.66, H 4.92, N 6.68. Found: C 49.16, H 5.164, N 5.90.

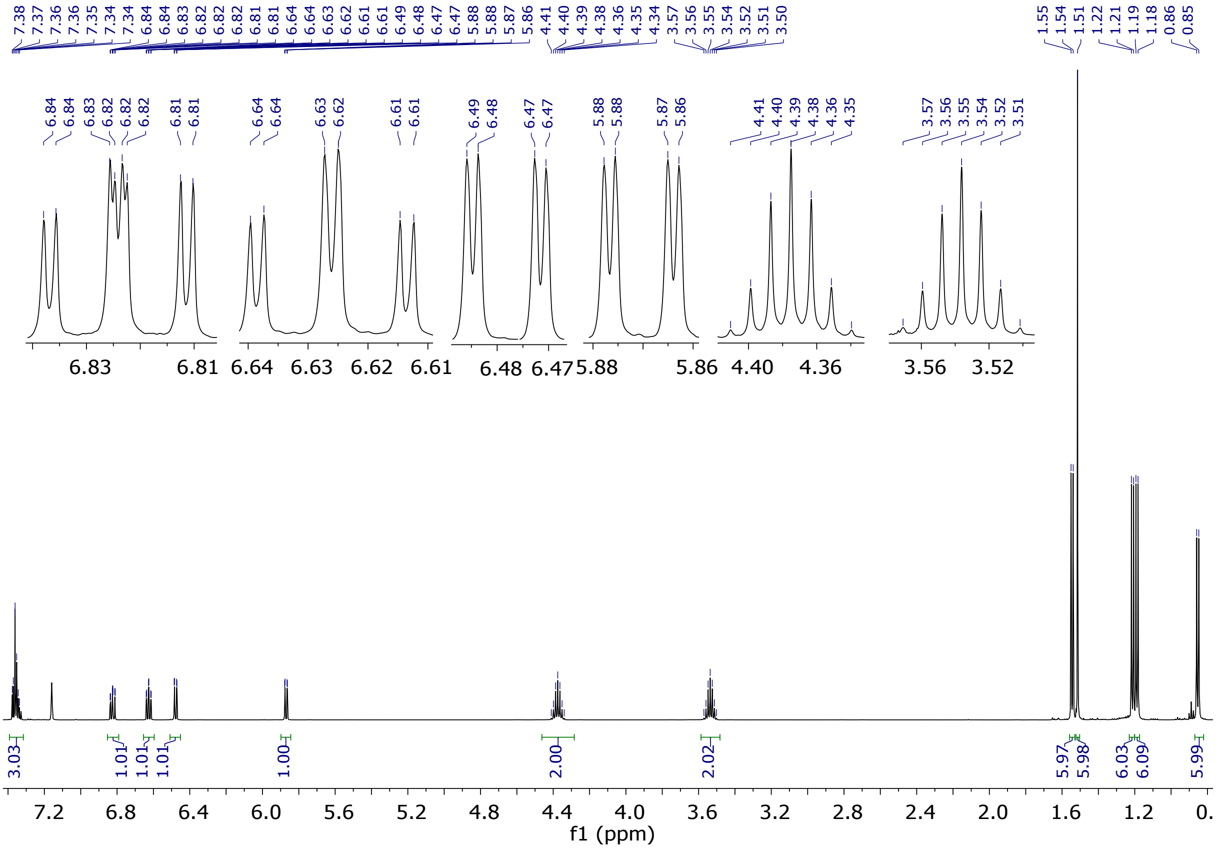

Figure S18: ^{1}H NMR spectrum of compound **8**, (600 MHz, C_6D_6, 25 °C).

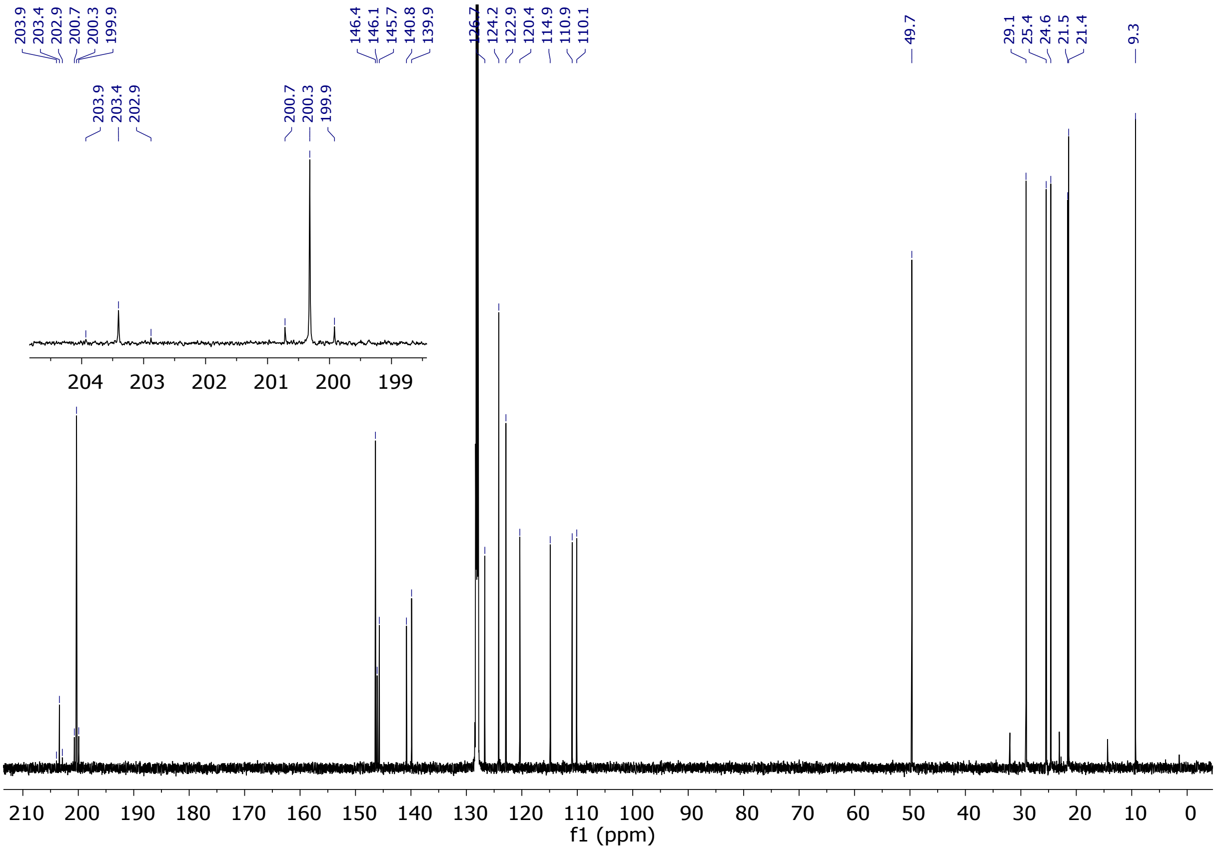

Figure S19: $^{13}C\{^{1}H\}$ NMR spectrum of compound **8**, (150 MHz, C_6D_6, 25 °C).

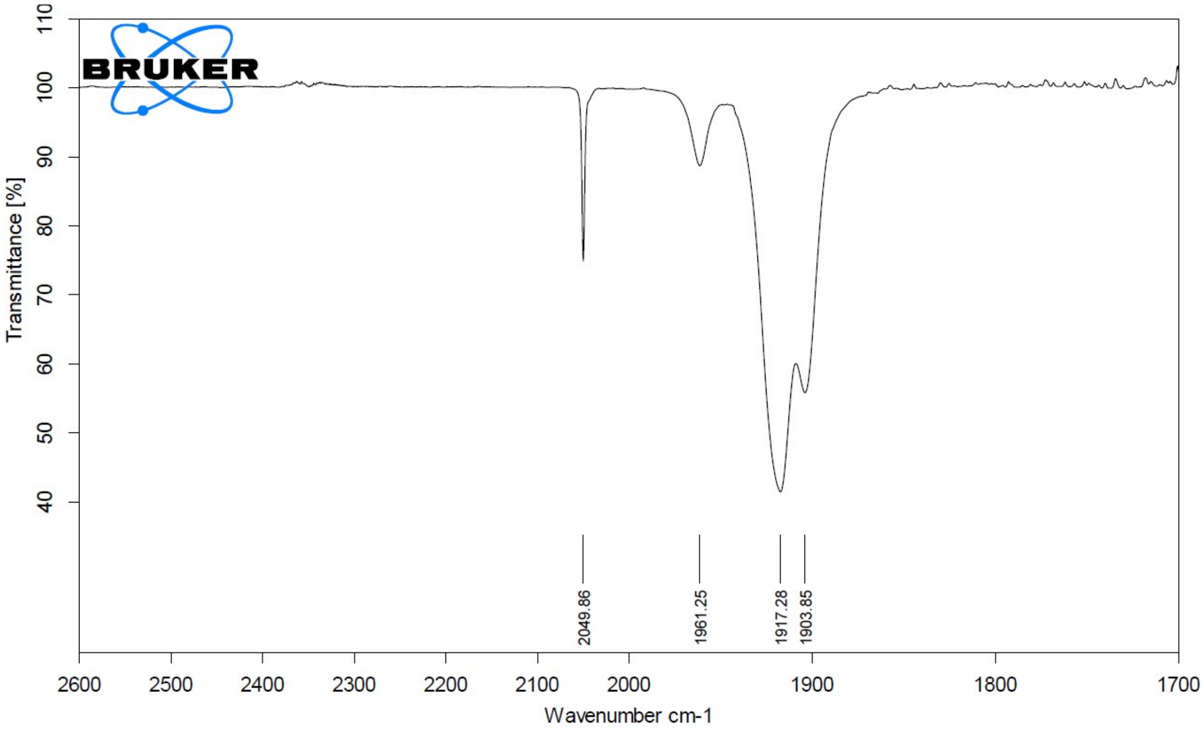

Figure S20: FT-IR spectrum of compound **8** in toluene.

2.9 AlI_2(AmIm) **10**

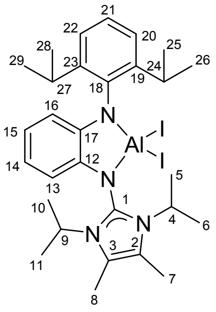

AlI_2(AmIm)

10

HAmIm **1** (1.00 g, 2.2 mmol, 1.0 eq.) was dissolved in toluene (40 mL) and *n*-BuLi (1.6 M in *n*-hexane, 1.40 mL, 2.2 mmol, 1.0 eq.) was added. The reaction was stirred for 30 min at 25 °C. AlI_3 (897 mg, 2.2 mmol, 1.0 eq.) was dissolved in toluene (20 mL) and added dropwise to the solution with formation of a colourless precipitate. After stirring for 2 h the solvent was removed *in vacuo* and the residue was dissolved in DCM (20 mL). The solution was filtered over Celite®. Layering with *n*-hexane (40 mL) and slow diffusion afforded product **10** (630 mg, 0.87 mmol, 40 %) as colourless crystals suitable for X-ray crystallography.

^{1}H NMR (300 MHz, CD_2Cl_2): δ (ppm) = 7.29 – 7.19 (m, 3 H, aryl C−*H* in Dipp), 6.61 – 6.50 (m, 1 H, C14−*H*), 6.37 (td, *J* = 7.5, 1.4 Hz, 1 H, C15−*H*), 5.90 (ddd, *J* = 7.9, 6.4, 1.4 Hz, 2 H, C13−*H*, C16−*H*), 5.02 (sept, *J* = 7.1 Hz, 2 H, NC*H*(CH_3)$_2$), 3.52 (sept, *J* = 6.8 Hz, 2 H, C*H*(CH_3)$_2$), 2.37 (s, 6 H, backbone C*H*$_3$), 1.64 (d, *J* = 7.0 Hz, 6 H, NCH(C*H*$_3$)$_2$), 1.39 (d, *J* = 7.0 Hz, 6 H, NCH(C*H*$_3$)$_2$), 1.26 (d, *J* = 6.9 Hz, 6 H, CH(C*H*$_3$)$_2$), 0.97 (d, *J* = 6.8 Hz, 6 H, CH(C*H*$_3$)$_2$).

^{13}C{^{1}H} NMR (75 MHz, CD_2Cl_2): δ (ppm) = 148.3 (s, *C*19, *C*23), 145.4 (s, *C*1), 144.4 (s, *C*12), 139.5 (s, *C*17), 138.6 (s, *C*18), 126.4 (s, *C*21), 124.7 (s, *C*20, *C*22), 124.1 (s, *C*2, *C*3), 121.0 (s, *C*14), 115.3 (s, *C*15), 113.1 (s, *C*16), 112.8 (s, *C*13), 50.4(s, *C*4, *C*9), 28.6 (s, *C*24, *C*27), 25.9, 25.7 (both s, *C*25, *C*26, *C*28, *C*29), 23.4, 21.6 (both s, *C*5, *C*6, *C*10, *C*11), 10.6 (s, *C*7, *C*8).

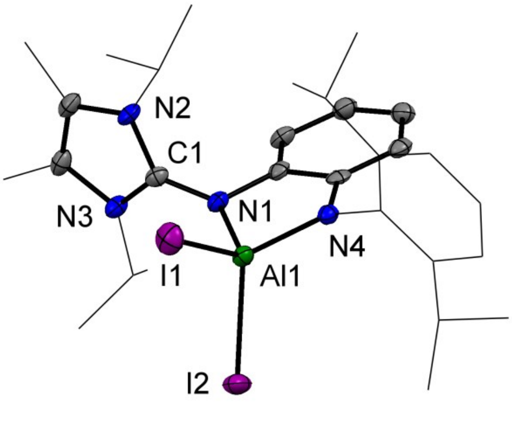

Figure S21: Molecular structure of **10**. Hydrogen atoms omitted. Thermal ellipsoids are presented at the 50 % level of probability. Bond distances and bond angles are reported in Å or degree (°), respectively: Al1−I1 2.5161(10), Al1−I2 2.5424(10), Al1−N4 1.829(3), Al1−N1 1.859(3), N1−C1 1.367(4), N1−Al1−N4 89.64(13), I1−Al1−N4 116.07(10), I1−Al1−N1 114.50(10).

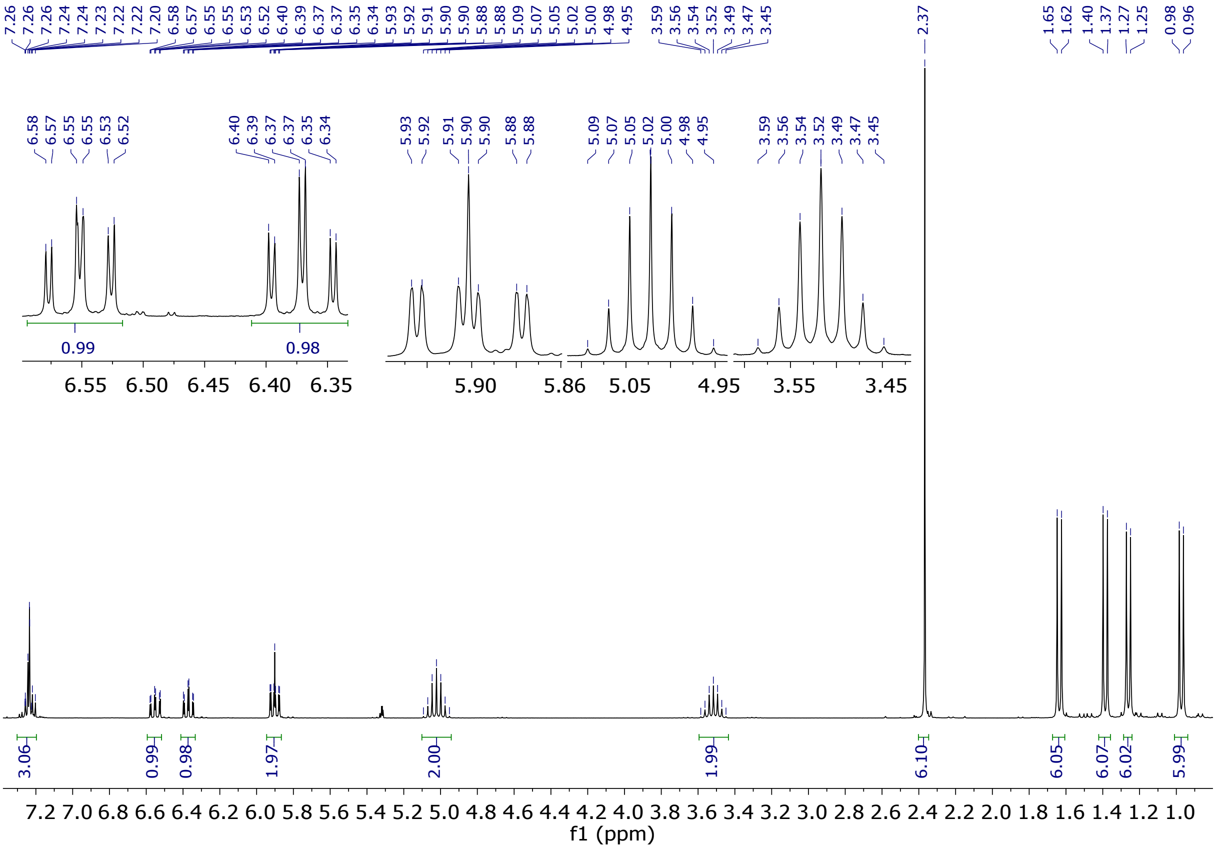

Figure S22: ^{1}H NMR spectrum of compound **10** (300 MHz, CD_2Cl_2, 25 °C).

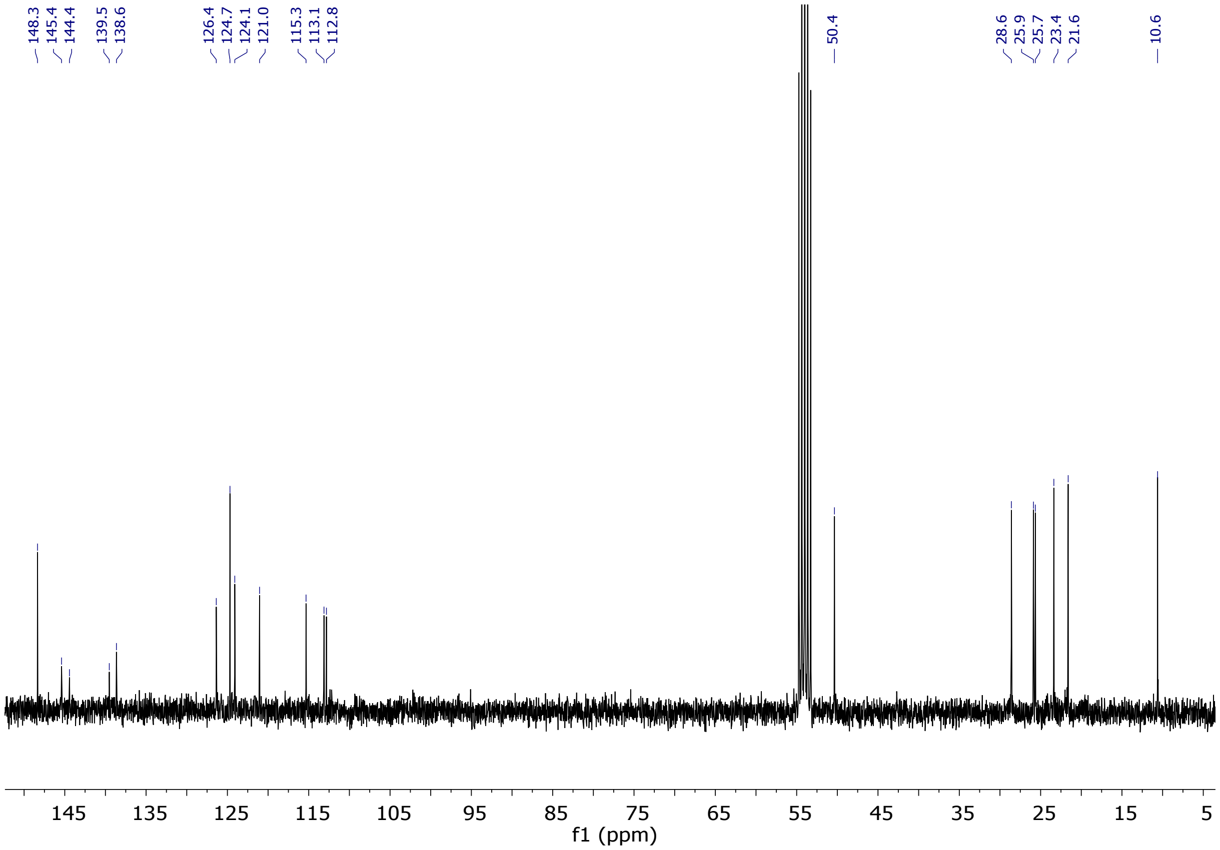

Figure S23: $^{13}C\{^1H\}$ NMR spectrum of compound **10** (75 MHz, CD_2Cl_2, 25 °C).

2.10 Compound **11**

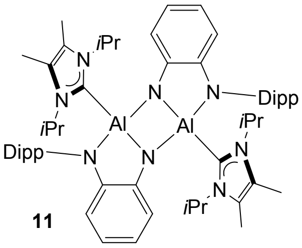

11

HAmIm **1** (200 mg, 0.448 mmol, 1.0 eq.) was dissolved in toluene (40 mL) and $NaCH_2SiMe_3$ (50 mg, 0.448 mmol, 1.0 eq.) was added. The reaction was stirred for 30 min at 25 °C. $(AlCp^*)_4$ (73 mg, 0.112 mmol, 0.25 eq.) was added, and the yellowish solution was stirred for 24 h with formation of a colourless precipitate. The filtrate was reduced to ca. 0.5 mL *in vacuo*. Slow solvent diffusion of n-pentane gave few colourless crystals of compound **11** suitable for X-ray crystallography.

3 X-ray Crystallography

Data collections were performed by mounting single crystals on glass fibers or MiTeGen mounts in perfluorinated oil. Diffractometers used for intensity measurements (at 100 K) were Oxford Diffraction Xcalibur E with Mo K_α radiation or Rigaku XtaLab Synergy S Single Source with either Mo K_α or Cu K_α micro source. Absorption correction was applied based on multi-scan methods. Data reduction was performed using the program CrysalisPro.[11] The structures were solved with SHELXT-14/5 [12] and refined anisotropically on F^2 using the programs SHELXL-14/7 and SHELXL-17/1.[13]

3.1 X-ray Crystallographic Details

Table S1: Crystallographic data for compound **1** and **6**.

Compound	HAmIm **1**	Tl(AmIm) **6**
CCDC entry code	2051403	2051408
Empirical formula	$C_{29}H_{42}N_4$	$C_{29}H_{41}N_4Tl$
Formula weight	446.66 [g · mol^{-1}]	650.03 [g · mol^{-1}]
Temperature	100(2) K	101(2) K
Wavelength	1.54184 Å	0.71073 Å
Crystal system	Triclinic	Monoclinic
Space group	$P\bar{1}$	$P2_1/n$
a	9.2682(3) Å	17.04920(10) Å
b	11.9420(2) Å	9.38140(10) Å
c	12.8815(3) Å	18.44040(10) Å
α	72.119(2)°	90°
β	75.806(2)°	107.6300(10)°
γ	85.257(2)°	90°
Volume	1315.35(6) Å^3	2810.93(4) Å^3
Z	2	4
Density (calculated)	1.128 g/cm^3	1.536 g/cm^3
Absorption coefficient	0.506 mm^{-1}	5.769 mm^{-1}
F(000)	488	1296
Crystal size	0.299 x 0.190 x 0.164 mm^3	0.209 x 0.132 x 0.056 mm^3
Theta range for data collection	3.707 to 74.504	2.461° to 34.139°
Reflections collected	76016	524677
Independent reflections	5520 [R(int) = 0.0292]	11088 [R(int) = 0.0779]
Goodness-of-fit on F^2	1.022	1.094
R1 [$I > 2\sigma(I)$]	0.0398	0.0299
wR2	0.1021	0.0560
Structure determination	Lars Denker	Lars Denker

Table S2: Crystallographic data for compound **4** and **5**.

Compound	In(AmIm) **5**	Ga(AmIm) **4**
CCDC entry code	2051405	2051404
Empirical formula	$C_{29}H_{41}N_4In$	$C_{29}H_{41}N_4Ga$
Formula weight	560.48 [g · mol^{-1}]	515.38 [g · mol^{-1}]
Temperature	100(2) K	100(2) K
Wavelength	1.54184 Å	0.71073 Å
Crystal system	Monoclinic	Monoclinic
Space group	$P2_1/c$	$C2/c$
a	17.06791(19) Å	29.0327(7) Å
b	9.46993(3) Å	9.5324(2) Å
c	28.6790(3) Å	20.7873(6) Å
α	90°	90°
β	142.490(2)°	96.762(2)°
γ	90°	90°
Volume	2822.49(10) Å^3	5712.9(2) Å^3
Z	4	8
Density (calculated)	1.319 g/cm^3	1.198 g/cm^3
Absorption coefficient	6.849 mm^{-1}	50.985 mm^{-1}
F(000)	1168	2192
Crystal size	0.138 x 0.116 x 0.059 mm^3	0.233 x 0.138 x 0.135 mm^3
Theta range for data collection	3.091 to 77.581°	2.490° to 26.370°
Reflections collected	218768	66758
Independent reflections	5963 [R(int) = 0.0360]	5829 [R(int) = 0.075]
Goodness-of-fit on F^2	1.056	1.034
R1 [$I > 2\sigma(I)$]	0.0266	0.0399
wR2	0.0708	0.0893
Structure determination	Lars Denker	Lars Denker

Table S3: Crystallographic data for compound **7** and **10**.

Compound	[Fe(CO)$_4${Ga(AmIm)}] **7**	AlI$_2$(AmIm) **10**
CCDC entry code	2051409	2051406
Empirical formula	$C_{33}H_{41}FeGaN_4O_4$	$C_{29}H_{41}AlI_2N_4$
Formula weight	683.27 [g · mol^{-1}]	726.44 [g · mol^{-1}]
Temperature	100(2) K	100(2) K
Wavelength	0.71073 Å	0.71073 Å
Crystal system	Monoclinic	Triclinic
Space group	*C2/c*	*P*–1
a	21.5254(2) Å	10.7878(5) Å
b	10.26190(10) Å	11.4686(5) Å
c	30.7840(3) Å	13.0738(4) Å
α	90°	92.946(3)°
β	94.4300(10)°	94.350(3)°
γ	90°.	101.494(4)°
Volume	6779.61(11) Å^3	1576.83(11) Å^3
Z	8	2
Density (calculated)	1.339 g/cm^3	1.530 g/cm^3
Absorption coefficient	1.263 mm^{-1}	2.045 mm^{-1}
F(000)	2848	724
Crystal size	0.338 x 0.251 x 0.238 mm^3	0.193 x 0.114 x 0.057 mm^3
Theta range for data collection	2.918 to 37.642°	2.594 to 26.371°
Reflections collected	291598	63860
Independent reflections	17624 [R(int) = 0.0571]	6454 [R(int) = 0.0642]
Goodness-of-fit on F^2	1.039	1.071
R1 [$I > 2\sigma(I)$]	0.0316	0.0360
wR2	0.0817	0.1074
Structure determination	Lars Denker	Lars Denker

Table S4: Crystallographic data for compound **11**.

Compound	Compound **11**
CCDC entry code	2051407
Empirical formula	$C_{70}H_{94}N_8Al_2$
Formula weight	1101.49 [g · mol^{-1}]
Temperature	100(2) K
Wavelength	1.54184 Å
Crystal system	Monoclinic
Space group	*C*2/*c*
a	22.5974(2) Å
b	10.01899(9) Å
c	28.1598(3) Å
α	90°
β	100.7266(10)°
γ	90°
Volume	6264.05(10)Å^3
Z	4
Density (calculated)	1.168 g/cm^3
Absorption coefficient	0.778 mm^{-1}
F(000)	2384
Crystal size	0.093 x 0.068 x 0.056 mm^3
Theta range for data collection	3.195 to 77.622°
Reflections collected	62577
Independent reflections	6604 [R(int) = 0.0296]
Goodness-of-fit on F^2	1.025
R1 [$I > 2\sigma(I)$]	0.0369
wR2	0.0972
Structure determination	Lars Denker

4 Calculation of Buried Volume Values

The calculations of the buried volume for the Ga(I) species …

Ga(Giso): $\%V_{bur} = 25.1$

Ga(AmIm) **4**: $\%V_{bur} = 26.0$

Ga(NacNac): $\%V_{bur} = 32.6$

…was performed with the web-based tool SambVca [14] employing the following parameters:

Distance of the Ga to coordination centre: 2.28 Å

Radius of the sphere: 3.50 Å

Mesh integration value: 0.05

Hydrogen atoms included.

5 Computational Studies

Methods: The carbenoides E(Giso), E(AmIm) and E(NacNac) were optimized using the modern ωB97XD functional [15] with the triple-zeta 6-311G++** basis set on all atoms and def2-TZVP ECP on In or Tl (if present). E = B, Al, Ga, In, Tl. Boron was included in the calculations for the sake of completeness.

All calculations were performed using Gaussian 09 software (Gaussian 09, Revision D.01, M. J. Frisch, et al. Gaussian, Inc., Wallingford CT, 2016). We used ultrafine grid for DFT and standard optimization and convergence parameters as implemented in Gaussian 09. Bond indices, partial charges and orbital localization calculations using Foster-Boys approach [16] was performed using the Multiwfn Version 3.7 software. [17] Orbitals visualization was performed using the VMD version 1.9.3 software [18].

The carbenoides E(NacNac) for E = B, Al, Ga, In, Tl were previously calculated with a truncated N-phenyl NacNac ligand by Chen *et al*. [19] For the sake of better comparsion to these previous calculations we employed the same model compounds for type **C** carbenoides.

The file with the Cartesian coordianates (.xyz format) is provided for each studied system as a separate file.

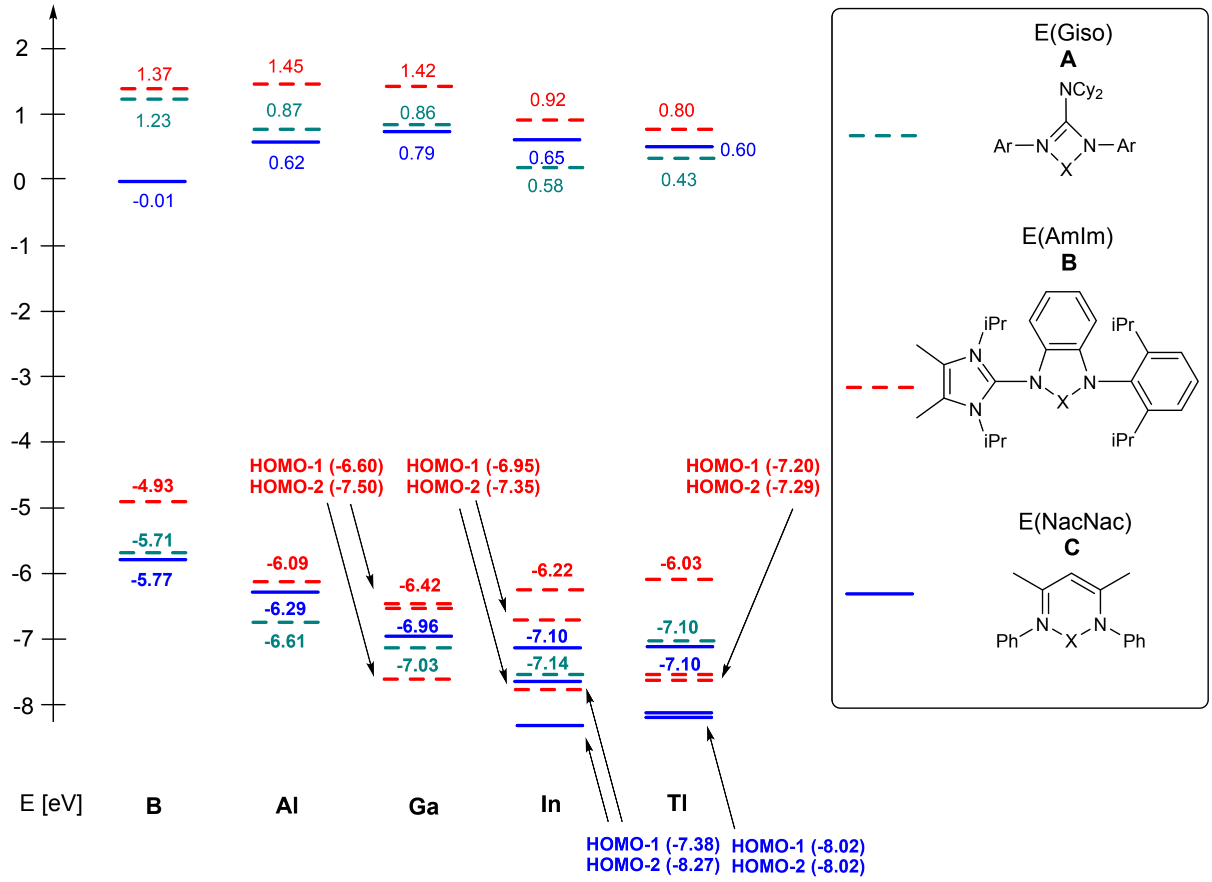

Figure S24: Frontier molecular orbitals of the carbenoides E(Giso), E(AmIm) and E(NacNac), E = B–Tl.

Table S5: Energies of the selected frontier orbitals (in eV)

System	X = B	X = Al	X = Ga	X = In	X = Tl
NacNac (**C**)					
HOMO-2	-8.59	-8.67	-8.48	-8.27	-8.02
HOMO-1	-8.25	-7.89	-7.69	-7.38	-8.02
HOMO	-5.76	-6.29	-6.96	-7.38	-7.10
LUMO	-0.01	0.62	0.79	0.65	0.60
LUMO+1	1.71	1.03	1.00	0.97	1.20
LUMO+2	1.76	1.56	1.60	1.62	1.66
AmIm (**B**)					
HOMO-2	-7.66	-7.48	-7.50	-7.35	-7.29
HOMO-1	-6.90	-6.42	-6.60	-6.95	-7.20
HOMO	-4.79	-6.06	-6.42	-6.22	-6.03
LUMO	1.61	1.62	1.42	0.92	0.80
LUMO+1	2.34	1.79	1.59	1.63	1.55
LUMO+2	2.37	2.34	2.19	1.92	1.90
Giso (**A**)					
HOMO-2	-8.48	-8.21	-8.07	-7.93	-7.62
HOMO-1	-8.21	-8.07	-8.02	-7.85	-7.44
HOMO	-5.71	-6.61	-7.03	-7.14	-7.10
LUMO	1.23	0.87	0.86	0.58	0.43
LUMO+1	1.53	1.70	1.70	1.35	1.01
LUMO+2	1.71	1.71	1.71	1.68	1.56

The previously reported trend by Chen *et al.* [19] in the HOMO orbitals energetics for the NacNac system of type **C** employing our state-of-the-art method is identical: the energy of HOMOs decreases from B to In, but for Tl the HOMO is slightly higher in energy. In the case of the new AmIm system the energy of HOMOs go falls from B to Ga, but then is slightly higher for In and Tl system. The analysis of frontier orbitals reveals two different sets of orbitals. For

NacNac type systems **C** in the cases of B, Al and Ga as well as for AmIm type systems **B** for the B and Al cases the HOMOs are located mostly on the triel atom akin to the previous findings suggesting a nonbonding sigma orbital of the lone pair of triel atom. For NacNac type systems **C** in the cases of In and Tl as well as for AmIm systems in the cases of Ga, In and Tl, however, the HOMOs are located mostly on the five/six-membered rings. For these systems molecular orbitals located mostly on triel atoms are now shifted and become either HOMO-1 [for In(NacNac), Ga(AmIm), In(AmIm)] or a combination of even lower lying HOMOs [Tl(NacNac), Tl(AmIm)]. See also the frontier orbitals visualization below.

The trend in LUMOs energetics is, on the other hand, quite different from Chen's findings. We observe a large raise in energy from B(NacNac) to Al(NacNac), but the differences between all other LUMOs are marginal. For the AmIm of type **B** system there is no simple trend and the energies of all LUMOs become similar. The analysis of the shapes of frontier orbitals shows that for B(NacNac), In(NacNac) and Tl(NacNac) as well as for Al(AmIm), Ga(AmIm), In(AmIm) and Tl(AmIm) the LUMO can be attributed to the p_z-orbital. In all other cases we also see a shift in the orbitals, which is in particular the LUMO+1 for Al(NacNac) and Ga(NacNac) and B(AmIm). These results are in partial agreement with Chen's results. Noteworthy, for the system with heavier X element the differences in HOMO-1 and HOMO and/or LUMO and LUMO+1 become smaller, and we do not observe a consistent pattern in the frontier orbitals akin to the Chen´s findings.

Table S6: Relative Energies for Singlet and Triplet Group 13 Carbenoides (in kcal/mol).

System	X = B	X = Al	X = Ga	X = In	X = Tl
NacNac (**C**)	-3.2	49.7	51.6	54.9	53.2
AmIm (**B**)	19.1	55.0	72.6	70.0	54.5
Giso (**A**)	17.2	51.0	68.9	73.0	62.0

Chen predicted that for the B(NacNac) system the singlet state is more stable than the triplet by 3.5 kcal/mol using B3LYP and a relatively small basis set. Our calculations using ωB97XD functional and triple zeta basis set predict the triplet to be more stable by 3.2 kcal/mol, see Table S6. Interestingly, using the same large basis set but the B3LYP functional we estimate the singlet to be more stable by ca. 1.8 kcal/mol. However, the conclusion from Chen's paper still holds stating the small singlet-triplet splitting energy in the case of boron, which strongly implies that this species is too unstable to be detected experimentally.

For the new hypothetical compound B(AmIm) a relatively large singlet-triplet splitting energy (19.1 kcal/mol) is predicted, suggesting that the singlet state should be stable. The values from Table S6 may be compared to the values for model carbenes, which form stable singlet states and show singlet-triplet splitting energies of 60−80 kcal/mol.[20]

Table S7: HOMO-LUMO gaps (in eV).

System	X = B	X = Al	X = G	X = In	X = Tl
NacNac (**C**)	5.75	6.91	7.75	8.03	7.71
AmIm (**B**)	6.30	7.52	7.85	7.14	6.83
Giso (**A**)	6.94	7.48	7.89	7.71	7.53

The HOMO-LUMO gaps for all studied systems are significant and lie above 5.7 eV, suggesting also high stabilities of all studied systems akin to stable carbene monomers and dimers, cf. [21] . The trends here are very similar for all three classes of compounds.

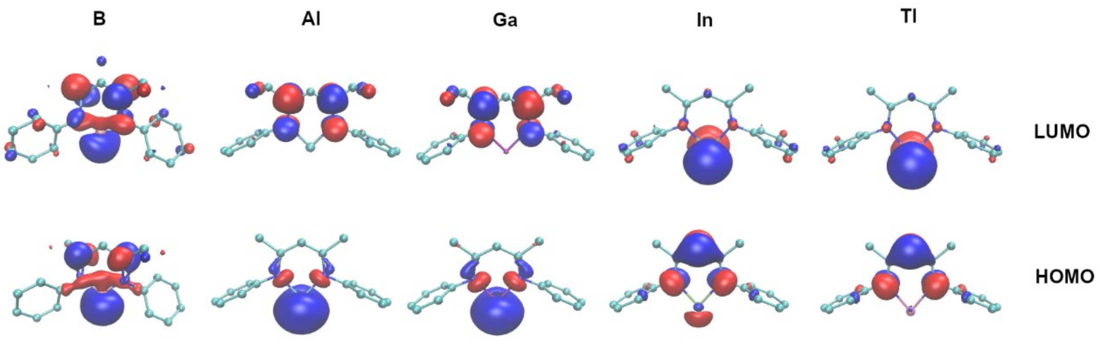

Figure S25: Frontier molecular orbitals for NacNac systems of type **C**.

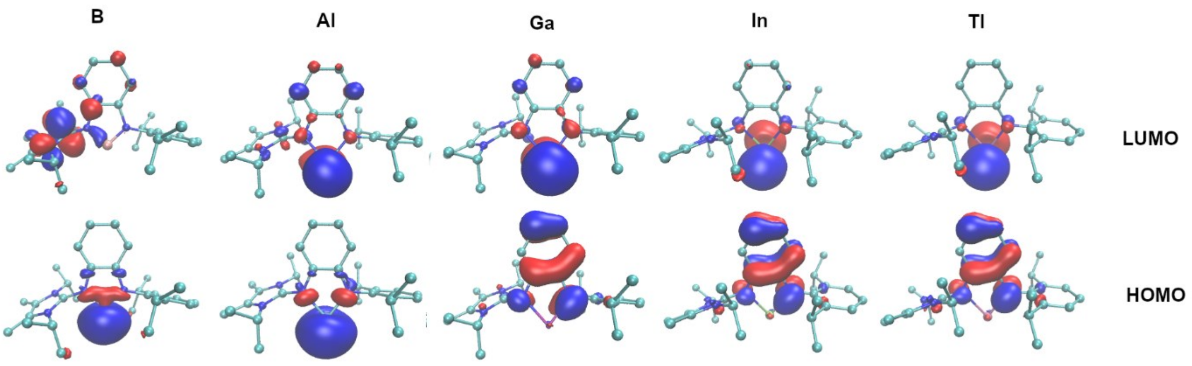

Figure S26: Frontier molecular orbitals for the new AmIm systems of type **B**.

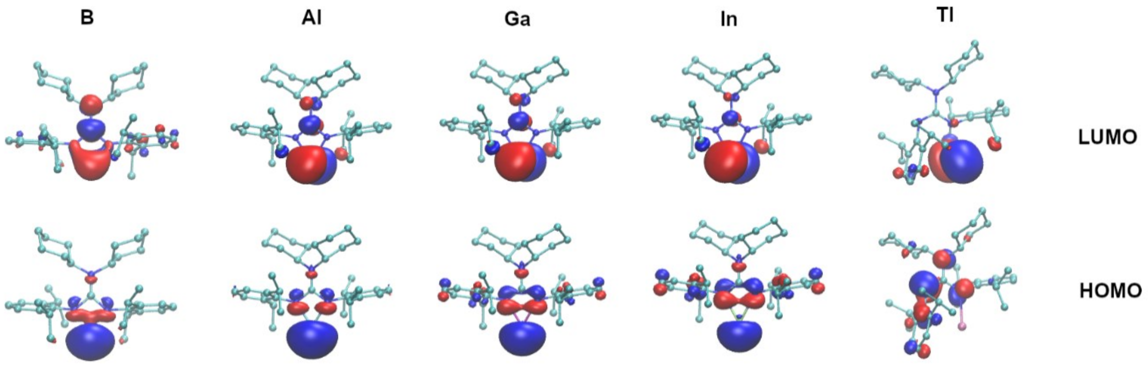

Figure S26: Frontier molecular orbitals for the Giso systems of type **A**.

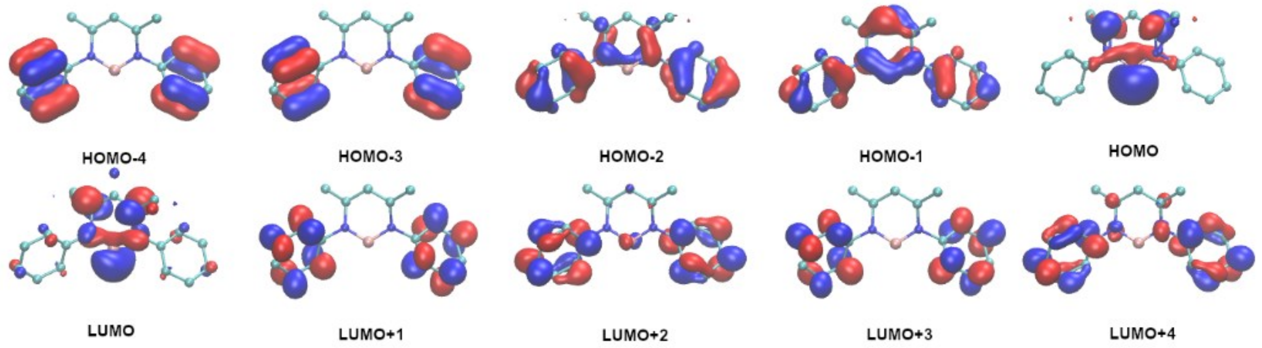

Figure S28: Frontier molecular orbitals for B(NacNac).

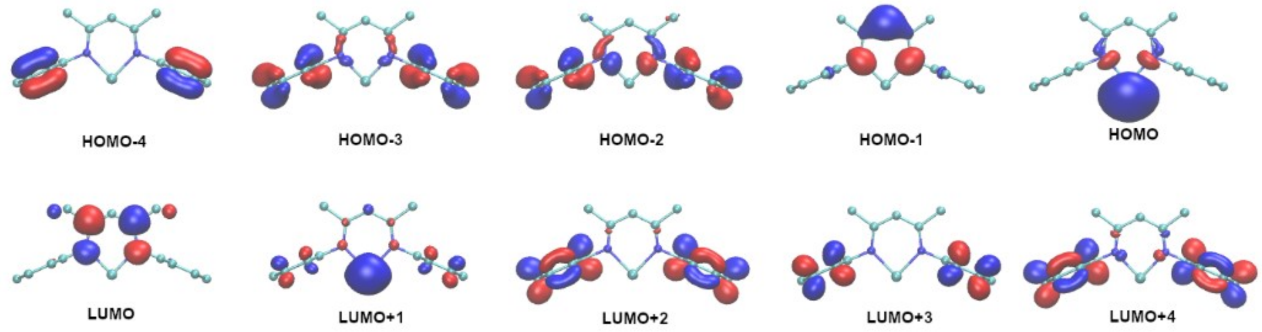

Figure S29: Frontier molecular orbitals for Al(NacNac).

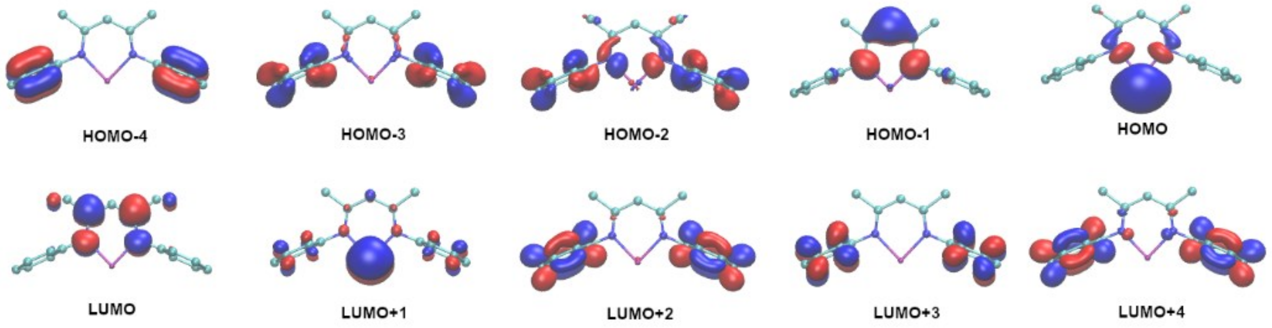

Figure S30: Frontier molecular orbitals for Ga(NacNac).

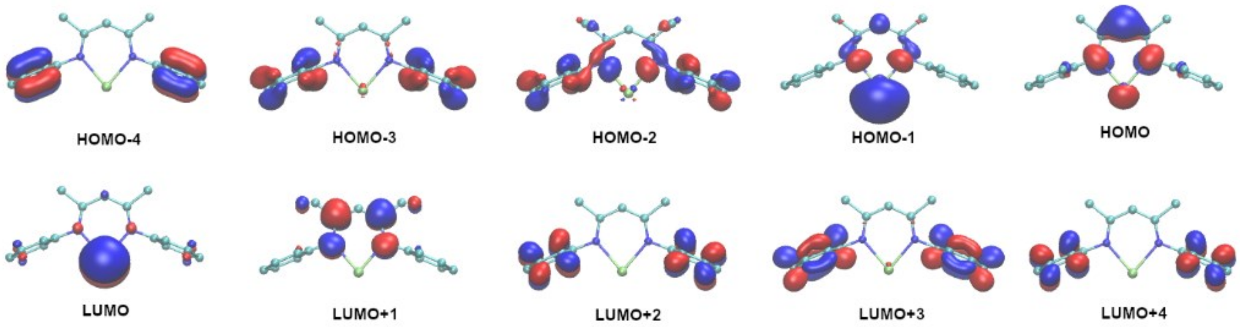

Figure S31: Frontier molecular orbitals for In(NacNac).

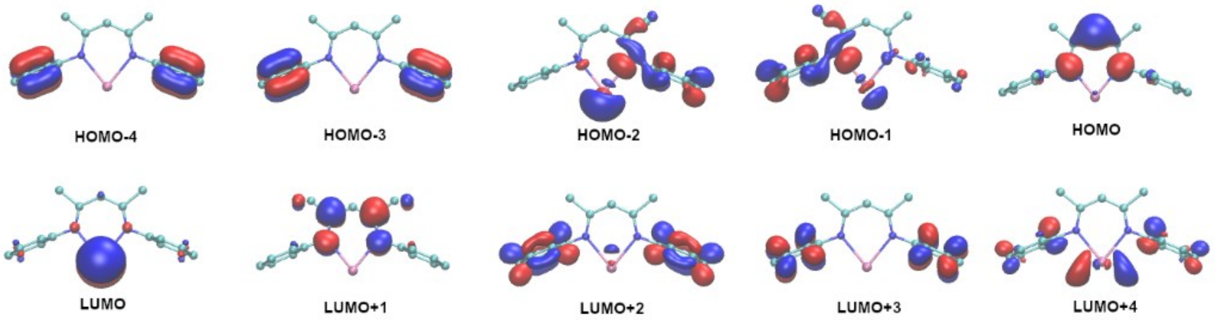

Figure S32: Frontier molecular orbitals for Tl(NacNac).

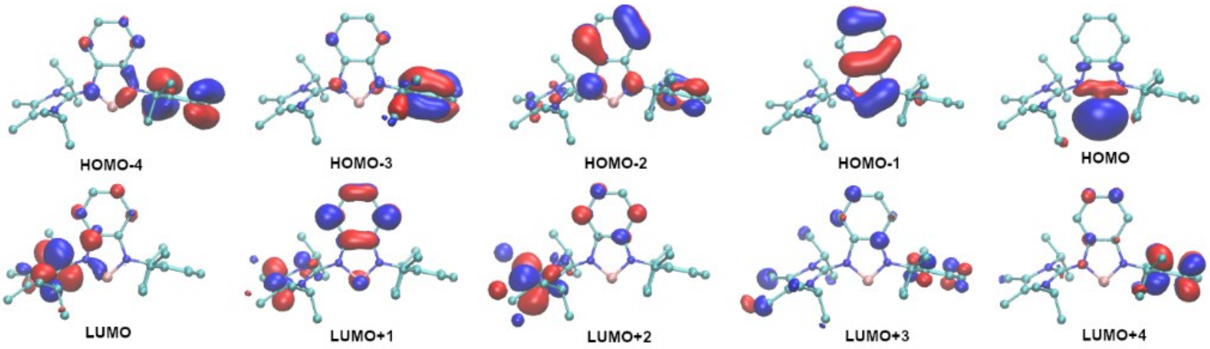

Figure S33: Frontier molecular orbitals for B(AmIm).

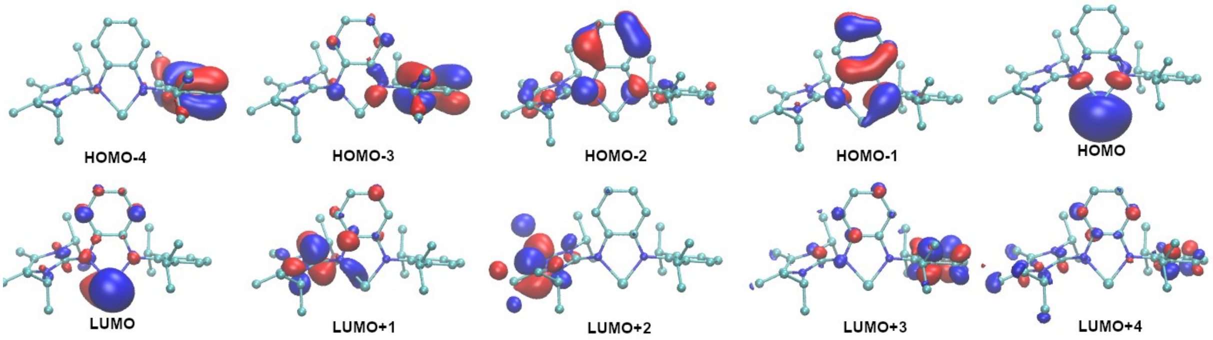

Figure S34: Frontier molecular orbitals for Al(AmIm).

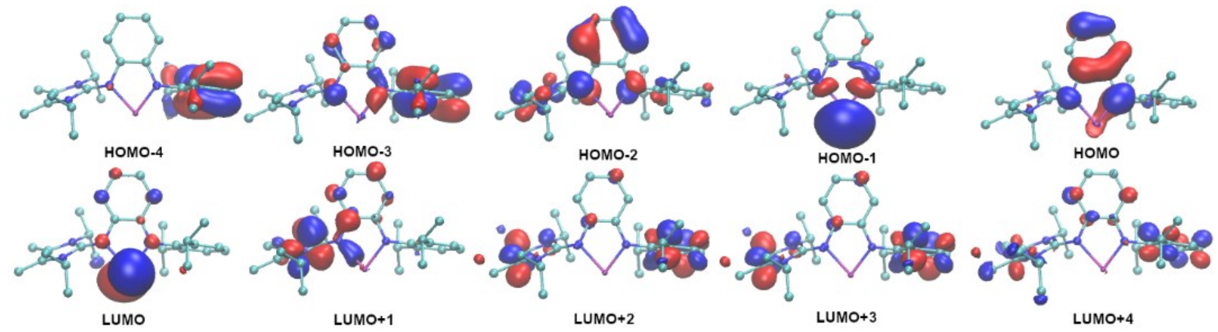

Figure S35: Frontier molecular orbitals for Ga(AmIm).

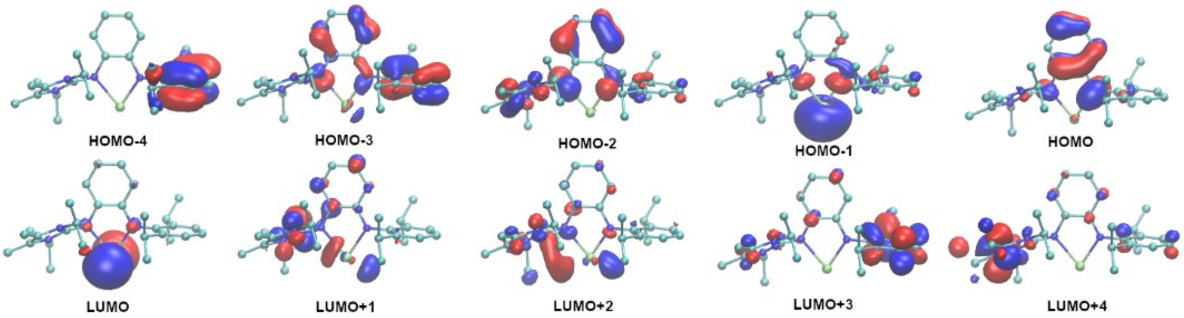

Figure S36: Frontier molecular orbitals for In(AmIm).

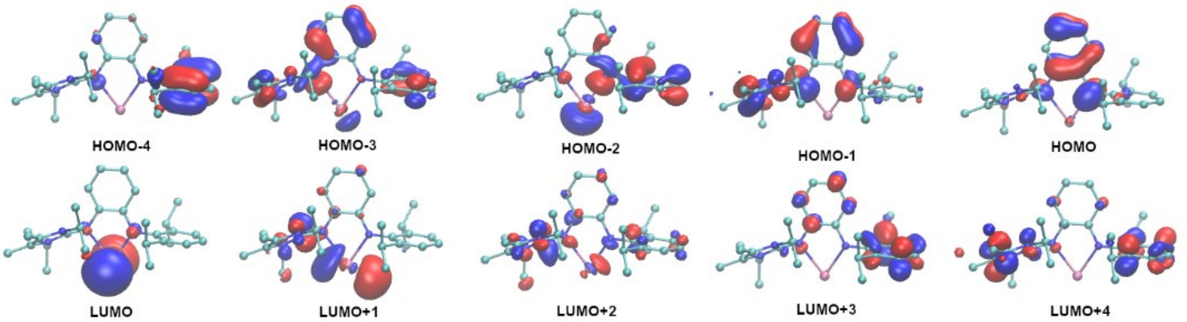

Figure S37: Frontier molecular orbitals for Tl(AmIm).

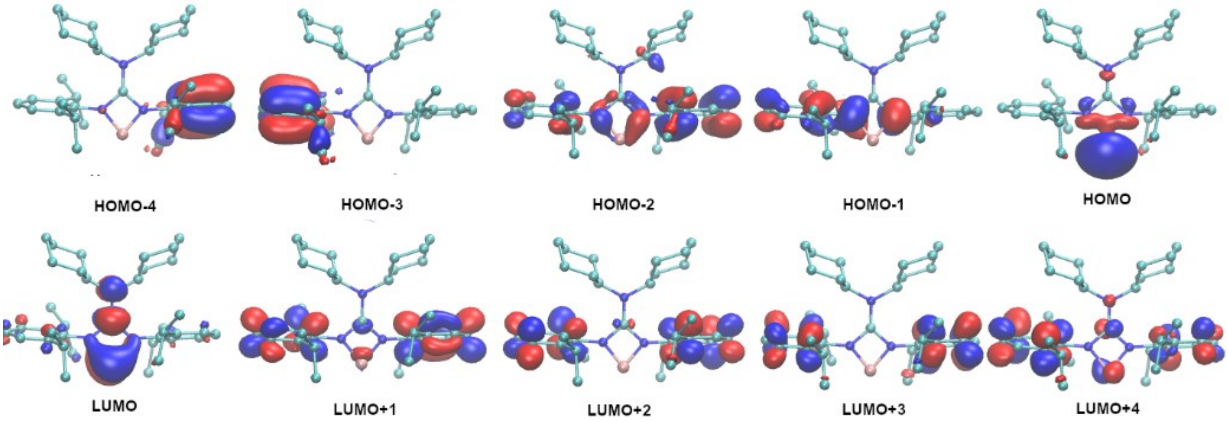

Figure S38: Frontier molecular orbitals for B(Giso).

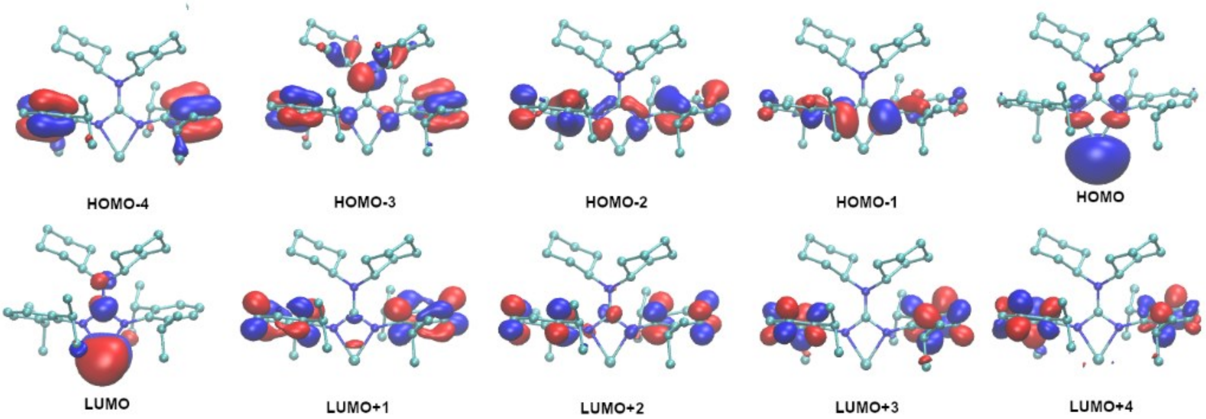

Figure S39: Frontier molecular orbitals for Al(Giso).

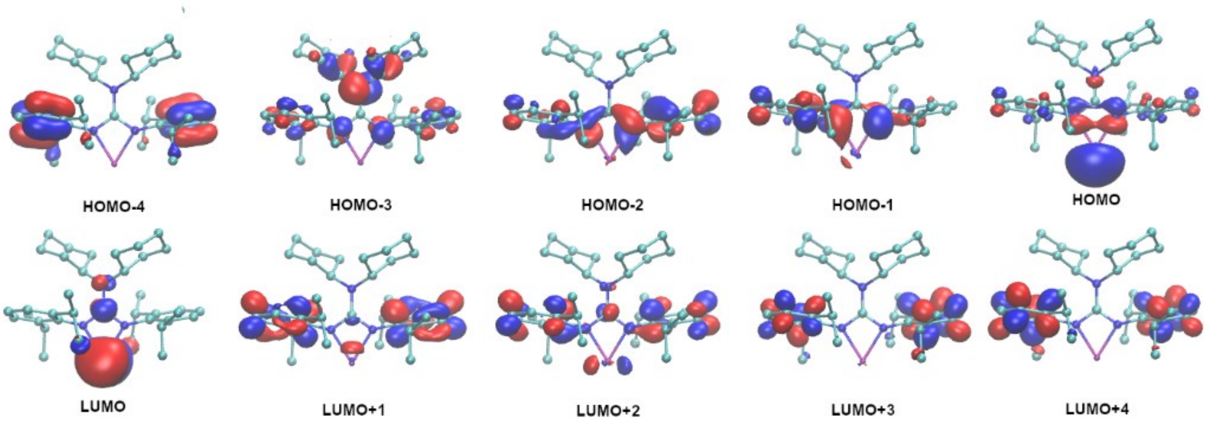

Figure S40: Frontier molecular orbitals for Ga(Giso).

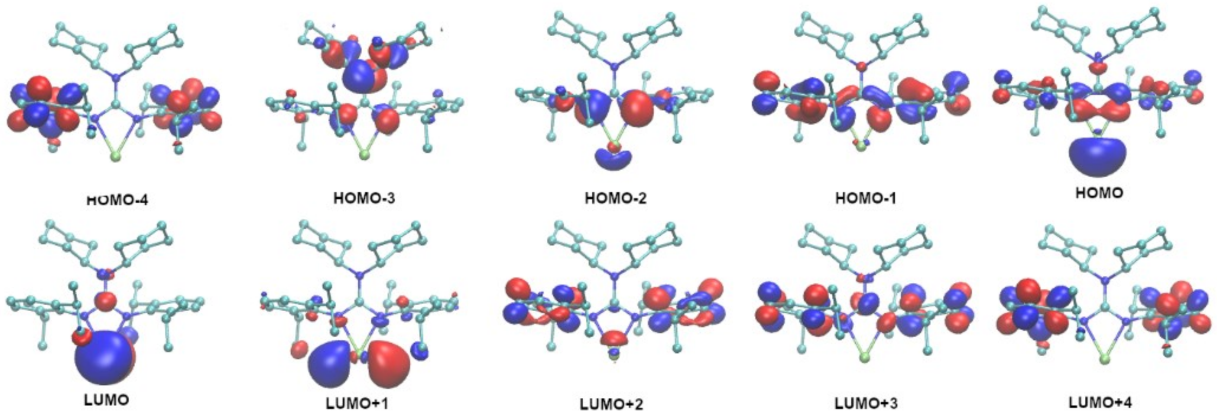

Figure S41: Frontier molecular orbitals for In(Giso).

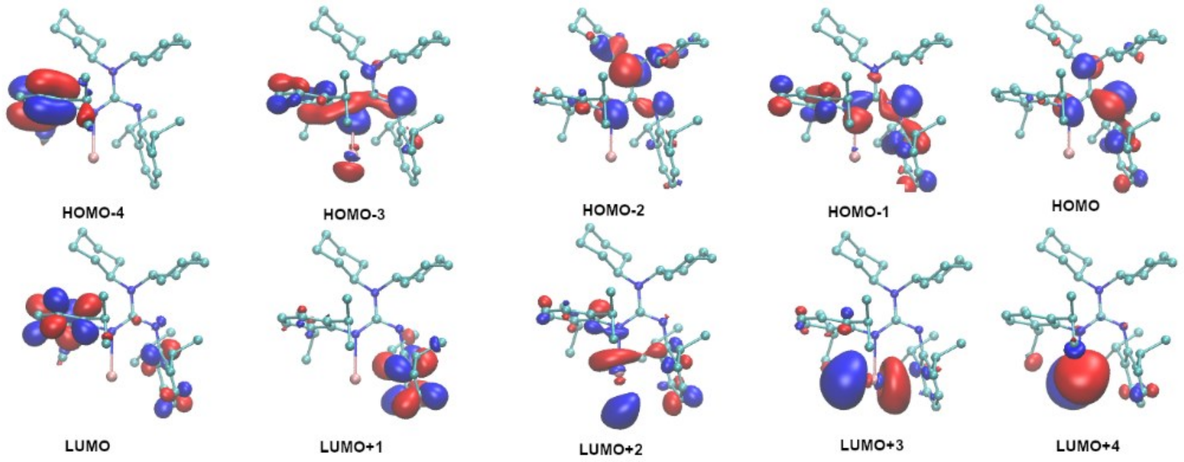

Figure S42: Frontier molecular orbitals for Tl(Giso).

6 References

[1] O. T. Beachley, J. C. Pazik, T. E. Glassman, M. R. Churchill, J. C. Fettinger, R. Blom, *Organometallics* **1988**, *7*, 1051–1059.
[2] P. Jutzi, L. O. Schebaum, *J. Organomet. Chem.* **2002**, *654*, 176–179.
[3] C. Ganesamoorthy, S. Loerke, C. Gemel, P. Jerabek, M. Winter, G. Frenking, R. A. Fischer, *Chem. Commun.* **2013**, *49*, 2858–2860.
[4] A. F. Neto, A. D. L. Borges, J. Miller, V. A. Darin, *Synth. React. Inorg. Met. Chem.* **1997**, *27*, 1299–1314.
[5] F. J. Arnáiz, *J. Chem. Educ.* **1997**, *74*, 1332–1333
[6] P. J. Bailey, R. A. Coxall, C. M. Dick, S. Fabre, L. C. Henderson, C. Herber, S. T. Liddle, D. Loroño-González, A. Parkin, S. Parsons, *Chem. - A Eur. J.* **2003**, *9*, 4820–4828.
[7] N. Kuhn, T. Kratz, *Synthesis (Stuttg).* **1993**, 561–562.
[8] H. Liu, M. Khononov, N. Fridman, M. Tamm, M. S. Eisen, *Inorg. Chem.* **2017**, *56*, 3153–3157.
[9] E. Merişor, U. Beifuss, *Tetrahedron Lett.* **2007**, *48*, 8383–8387.
[10] R. A. Kunetskiy, I. Císařová, D. Šaman, I. M. Lyapkalo, *Chem. - A Eur. J.* **2009**, *15*, 9477–9485.
[11] Rigaku Oxford Diffraction, *"CrysAlisPRO Softw. Syst. version 1.171.39.46"* **2018**, Rigaku Corporation, Oxford, UK. (Ed.).
[12] G. M. Sheldrick, *Acta Cryst.* **2015**, *A71*, 3–8.
[13] G. M. Sheldrick, *Acta Crystallogr., Sect. A Found. Crystallogr.* **2008**, *64*, 112–122.
[14] L. Falivene, Z. Cao, A. Petta, L. Serra, A. Poater, R. Oliva, V. Scarano, L. Cavallo, *Nat. Chem.* **2019**, *11*, 872–879. https://www.molnac.unisa.it/OMtools/sambvca2.1/index.html.
[15] J.-D. Chai, M. Head-Gordon, *Phys. Chem. Chem. Phys.* **2008**, *10*, 6615–6620.
[16] J. M. Foster, M. F. Boys, *Rev. Mod. Phys.* **1960**, *32*, 300–302.
[17] T. Lu, F. Chen, *J. Comput. Chem.* **2012**, 33, 580−592.
[18] W. Humphrey, A. Dalke, K. Schulten, *J. Mol. Graph.* **1996**, *14*, 33−38.
[19] C.-H. Chen, M.-L. Tsai, M.-D. Su, *Organometallics* **2006**, 25, 2766−2773.
[20] a) C. Heinemann, W. Thiel, *Chem. Phys. Lett.* **1994**, *217*, 11–16; b) E. A. Carter, W. A. Goddard, *J. Phys. Chem.* **1986** *,90*, 998–1001
[21] K. Młodzikowska, A. A. Rajkiewicz, K. Grela, B. Trzaskowski, *New J. Chem.* **2018**, *42*, 6183−6190.